

A DEEP LEARNING ALGORITHM FOR HIGH-DIMENSIONAL EXPLORATORY ITEM FACTOR ANALYSIS

CHRISTOPHER J. URBAN AND DANIEL J. BAUER

UNIVERSITY OF NORTH CAROLINA AT CHAPEL HILL

July 21, 2022

This material is based upon work supported by the National Science Foundation Graduate Research Fellowship under Grant No. DGE-1650116.

We would like to thank to the Editor, the Associate Editor, and the reviewers for their many constructive comments. We are also grateful to Dr. David Thissen for his extensive suggestions, feedback, and support.

Correspondence should be sent to cjurban@live.unc.edu.

A DEEP LEARNING ALGORITHM FOR HIGH-DIMENSIONAL EXPLORATORY ITEM FACTOR ANALYSIS

Abstract

Marginal maximum likelihood (MML) estimation is the preferred approach to fitting item response theory models in psychometrics due to the MML estimator's consistency, normality, and efficiency as the sample size tends to infinity. However, state-of-the-art MML estimation procedures such as the Metropolis-Hastings Robbins-Monro (MH-RM) algorithm as well as approximate MML estimation procedures such as variational inference (VI) are computationally time-consuming when the sample size and the number of latent factors are very large. In this work, we investigate a deep learning-based VI algorithm for exploratory item factor analysis (IFA) that is computationally fast even in large data sets with many latent factors. The proposed approach applies a deep artificial neural network model called a variational autoencoder for exploratory IFA. An importance sampling technique to help the variational estimator better approximate the MML estimator is explored. We provide a real data application that recovers results aligning with psychological theory across random starts. Via simulation studies, we empirically demonstrate that the variational estimator is consistent (although factor correlation estimates exhibit some bias) and yields similar results to MH-RM in less time. Our simulations also suggest that the proposed approach performs similarly to and is potentially faster than constrained joint maximum likelihood estimation, a fast procedure that is

consistent when the sample size and the number of items simultaneously tend to infinity.

Key words:

Deep learning, artificial neural network, variational inference, variational autoencoder, importance sampling, importance weighted autoencoder, item response theory, categorical factor analysis, latent variable modeling

1. Introduction

Psychology and education researchers often collect large-scale test data with many respondents and many items in order to measure unobserved latent constructs such as personality traits or cognitive abilities. When test items are dichotomous (e.g., “Yes” or “No”) or polytomous (e.g., “Always”, “Frequently”, “Occasionally”, or “Never”), item factor analysis (IFA) is a principled alternative to linear factor analysis for summarizing the items using a smaller number of continuous latent factors. Exploratory IFA (Bock, Gibbons, & Muraki, 1988) in particular is an indispensable tool for uncovering the latent structure underlying a test by estimating the associations between items and latent factors (i.e., the factor loadings) in a data-driven manner. See Bolt (2005) or Wirth and Edwards (2007) for overviews of exploratory IFA.

Exploratory IFA parameters are most often estimated using Bock and Aitkin’s (1981) marginal maximum likelihood (MML) estimator, which enjoys consistency, normality, and efficiency as the sample size approaches infinity. The MML approach estimates the item parameters by maximizing the marginal likelihood of the observed item responses, which is obtained by integrating out the latent factors. Problematically, the computational complexity of evaluating this integral is exponential in the dimension of the latent space, making direct evaluation of the marginal likelihood computationally burdensome in the high-dimensional setting. A variety of methods for approximating the integrals have been proposed, including adaptive Gaussian quadrature (Rabe-Hesketh, Skrondal, & Pickles, 2005; Schilling & Bock, 2005), Laplace approximation (e.g., Huber, Ronchetti, & Victoria-Feser, 2004), Monte Carlo integration (e.g., Meng & Schilling, 1996; Song & Lee, 2005), Markov Chain Monte Carlo (e.g., Bguin & Glas, 2001; Edwards, 2010), and stochastic approximation (SA; e.g., Cai, 2010a; Cai, 2010b; Zhang, Chen, & Liu, 2020). The Metropolis-Hastings Robbins-Monro (MH-RM; Cai, 2010a; 2010b) SA algorithm has been particularly widely used in psychology and in education due to its computational

efficiency, and the recent stochastic expectation-maximization (stEM; Zhang, Chen, & Liu, 2020) algorithm performs comparably to MH-RM. However, even these state-of-the-art SA algorithms are computationally intensive when the sample size and the number of latent factors are very large.

Other marginal likelihood-based parameter estimation methods for exploratory IFA avoid computing high-dimensional integrals and are therefore more computationally efficient. Limited-information approaches such as the bivariate composite likelihood estimator (Jreskog & Moustaki, 2001) and the weighted least squares estimator (Muthn, 1978; 1984) yield fast, consistent, and asymptotically normally distributed estimates but are not asymptotically efficient. Approaches based on variational inference (VI; Jordan, Ghahramani, Jaakkola, & Saul, 1998; Wainwright & Jordan, 2008) perform approximate MML estimation by optimizing a lower bound on the marginal likelihood rather than the marginal likelihood itself. More specifically, VI posits a family of approximate latent variable (LV) posterior distributions, then finds the member of this family that is closest to the true LV posterior distribution by optimizing the aforementioned lower bound; the variational estimator is equivalent to the MML estimator when the approximate and true LV posterior distributions are precisely equal. Since a separate set of approximate LV posterior distribution parameters is estimated for each data point, VI’s computational complexity depends on the sample size and on the complexity of the approximating family. Variational methods for IFA have demonstrated competitive performance with SA algorithms such as MH-RM for small sample sizes (Hui, Warton, Ormerod, Haapaniemi, & Taskinen, 2017), although consistency of the variational estimator has not been proven for IFA (but see Hui, Warton, Ormerod, Haapaniemi, & Taskinen, 2017, for a heuristic proof).

The MML estimator’s computational inefficiency arises from treating the latent factors as random effects that must be integrated out of the marginal likelihood. An alternative class of computationally efficient estimators treats the latent factors as fixed parameters, thereby avoiding the need for specifying a prior distribution on the latent factors and for

evaluating high-dimensional integrals. However, these estimators pay a price for their computational efficiency: namely, they are only consistent in the double asymptotic setting where both the sample size and the number of items simultaneously tend to infinity. The constrained joint maximum likelihood estimator (CJMLE; Chen, Li, & Zhang, 2019) is the state-of-the-art estimator in this class; it is faster than MML-based approaches and is efficient in the double asymptotic setting. Zhang, Chen, and Li’s (2020) estimator based on singular value decomposition (SVD) is faster than CJMLE and does not suffer from convergence issues, although it is not (double) asymptotically efficient.

It is clear that an estimation procedure combining the asymptotic properties of the MML estimator with the computational efficiency of CJMLE is lacking from the IFA literature. In this work, we investigate a VI-based procedure that offers a step toward achieving these properties. This procedure employs techniques from two active deep learning (DL) research areas: amortized variational inference (AVI; Gershman & Goodman, 2014) and importance weighted variational inference (IWVI; Burda, Grosse, & Salakhutdinov, 2016; Domke & Sheldon, 2018). AVI modifies traditional VI by using a powerful function approximator called an inference model to predict the parameters of the LV posterior for each data point rather than estimating these parameters directly. AVI is faster than traditional VI for large data sets, although it can be less flexible in practice (Cremer, Li, & Duvenaud, 2018). IWVI decreases the gap between the variational lower bound and the true marginal likelihood by drawing multiple importance-weighted samples from the approximate LV posterior during fitting, typically trading computational efficiency for a better lower bound. When the number of importance-weighted samples equals infinity, IWVI is theoretically equivalent to MML estimation and thus inherits the asymptotic properties of the MML estimator (Burda, Grosse, & Salakhutdinov, 2016).

The proposed algorithm is based on the variational autoencoder (VAE; Kingma & Welling, 2014; Rezende, Mohamed, & Wierstra, 2014), an algorithm for AVI whose inference model is a deep artificial neural network (ANN). Our work extends that of Curi

et al. (2019), who used a VAE to estimate item parameters in a confirmatory multidimensional two-parameter logistic (M2PL) model. Our work is also related to concurrent work by Wu et al. (2020), who applied a VAE for confirmatory M2PL item parameter estimation in the Bayesian setting. Our contributions are as follows: (1) We apply the VAE to polytomous item response data in the frequentist setting; (2) we analyze the suitability of the VAE for exploratory rather than confirmatory IFA; (3) we introduce IWVI to the IFA literature by approximating the marginal log-likelihood using an importance sampling technique; and (4) we conduct simulation studies to investigate the asymptotic properties of the VAE and to compare the VAE to MH-RM and CJMLE.

Our paper is organized as follows. Section 2 provides a brief overview of ANNs. Section 3 introduces the problem of fitting IFA models with polytomous responses. Section 4 describes AVI and IWVI for IFA. The full algorithm is proposed in Section 5 and computational details are discussed. Section 6 includes an empirical example and simulation studies. Extensions of the method are described in Section 7 and discussions are given in Section 8.

2. A Brief Overview of Artificial Neural Networks

Deep learning (DL) models are machine learning models that map a set of predictor variables through a sequence of transformations called layers to predict a set of outcome variables. Much of DL’s success in recent years can be attributed to a family of nonlinear statistical models called artificial neural networks (ANNs; LeCun, Bengio, & Hinton, 2015). ANNs are essential building blocks for the algorithm described in this work.

2.1. Feedforward Neural Networks

Feedforward neural networks (FNNs) are a simple class of ANNs. In practice, they are used as powerful function approximators because they can approximate any Borel measurable function between finite dimensional spaces to any desired degree of accuracy

(Cybenko, 1989). Consider a data set $\{\mathbf{y}_i, \mathbf{x}_i\}_{i=1}^N$ where \mathbf{x}_i is the i^{th} observed $J \times 1$ vector of predictor variables and \mathbf{y}_i is the i^{th} observed $P \times 1$ vector of outcome variables. Note that here we define \mathbf{x}_i as a vector of observed variables in line with typical treatments of FNNs, although we will redefine it as a vector of LVs in Section 3. FNNs map the predictor variables through a sequence of L transformations to predict the outcome variables as follows:

$$\mathbf{h}_i^{(l)} = f^{(l)}(\mathbf{W}^{(l)}\mathbf{h}_i^{(l-1)} + \mathbf{b}^{(l)}), \quad l = 1, \dots, L, \quad (1)$$

where $\mathbf{h}_i^{(0)} = \mathbf{x}_i$, $\mathbf{h}_i^{(L)} = \mathbf{y}_i - \boldsymbol{\varepsilon}_i$ where $\boldsymbol{\varepsilon}_i$ is the i^{th} $J \times 1$ vector of errors, $\mathbf{h}_i^{(l)}$ is a $P_l \times 1$ vector of LVs for layers $l = 2, \dots, L-1$, $\mathbf{W}^{(l)}$ is a $P_l \times P_{l-1}$ matrix of regression weights for layer l , $\mathbf{b}^{(l)}$ is a $P_l \times 1$ vector of intercepts for layer l , and $f^{(l)}$ is an almost everywhere differentiable activation function for layer l . \mathbf{x}_i is called the input layer, $\mathbf{h}_i^{(1)}, \dots, \mathbf{h}_i^{(L-1)}$ are called hidden layers, and \mathbf{y}_i is called the output layer. Figure 1 shows an FNN schematic diagram.

=====
 Insert Figure 1 about here
 =====

Notice that FNNs are recursive generalized linear models where each activation function $f^{(l)}$ is an inverse link function linking a linear combination of the variables at layer $l-1$ to the mean of the variables at layer l . In this work, we set the hidden layer activation functions $f^{(1)}, \dots, f^{(L-1)}$ to the exponential linear unit (ELU) function

$$f(z) = \begin{cases} z, & \text{if } z \geq 0 \\ \exp(z) - 1, & \text{if } z < 0 \end{cases}, \quad z \in \mathbb{R}, \quad (2)$$

which is applied to vectors element-wise. FNNs with ELU hidden layer activation functions are easy to fit and perform well in practice (Clevert, Unterthiner, & Hochreiter, 2016). We

set the final activation function $f^{(L)}$ to the identity function:

$$f(z) = z, \quad z \in \mathbb{R}, \quad (3)$$

which is applied to vectors element-wise and corresponds to a linear regression of the layer $L - 1$ LVs on the outcomes.

2.2. Fitting FNNs Using AMSGrad

FNNs are typically fitted using stochastic gradient (SG) methods, a class of algorithms that iteratively update model parameters using stochastic estimates of the gradient of the objective function. Readers are referred to Bottou, Curtis, and Nocedal (2018) for an overview of SG methods. In this work, we use the AMSGrad SG algorithm (Reddi, Kale, & Kumar, 2018), a method that adapts the magnitudes of its parameter updates using exponential moving averages of past stochastic gradient estimates. This approach allows AMSGrad to dynamically utilize information from the observed data to update each parameter a different amount at each iteration (Duchi, Hazan, & Singer, 2011; McMahan & Streeter, 2010). AMSGrad has theoretical convergence guarantees and performs well in practice with little tuning. In contrast, approaches based on the Robbins-Monro SA algorithm require the user to pre-specify a sequence of parameter update magnitudes that are fixed across parameters at each fitting iteration. These pre-specified update schemes typically require fine-tuning to the observed data and are often unstable on implementation (Nemirovski, Juditsky, Lan, & Shapiro, 2009; Spall, 2005).

Let $\boldsymbol{\xi}_t$ be a $d \times 1$ vector of parameter values at fitting iteration t , $t = 0, \dots, T$, and let $\mathcal{J} : \mathbb{R}^d \mapsto \mathbb{R}$ be a possibly non-convex objective function that decomposes as a sum over observations:

$$\mathcal{J}(\boldsymbol{\xi}_t) = \frac{1}{N} \sum_{i=1}^N \mathcal{J}_i(\boldsymbol{\xi}_t), \quad (4)$$

where \mathcal{J}_i is a per-observation objective function. Let $\{\mathbf{y}_i, \mathbf{x}_i\}_{i=1}^M$ where $M < N$ be a subsample of observations called a mini-batch. Then at iteration t , an unbiased estimator of the gradient of the objective function for the full data set is

$$\mathbf{g}_t = \frac{1}{M} \nabla_{\boldsymbol{\xi}_t} \sum_{i=1}^M \mathcal{J}_i(\boldsymbol{\xi}_t), \quad (5)$$

where $\nabla_{\boldsymbol{\xi}_t}$ returns a $d \times 1$ vector of first-order partial derivatives w.r.t. $\boldsymbol{\xi}_t$. AMSGrad proposes iterative parameter updates as follows:

$$\boldsymbol{\xi}_{t+1} = \boldsymbol{\xi}_t - \eta \frac{\mathbf{m}_t}{\sqrt{\hat{\mathbf{v}}_t}}, \quad (6)$$

where

$$\begin{aligned} \mathbf{m}_t &= \beta_1 \mathbf{m}_{t-1} + (1 - \beta_1) \mathbf{g}_t; \\ \mathbf{v}_t &= \beta_2 \mathbf{v}_{t-1} + (1 - \beta_2) \mathbf{g}_t^2; \\ \hat{\mathbf{v}}_t &= \max(\hat{\mathbf{v}}_{t-1}, \mathbf{v}_t); \end{aligned} \quad (7)$$

$\mathbf{m}_0 = \mathbf{0}$; $\mathbf{v}_0 = \mathbf{0}$; $\hat{\mathbf{v}}_0 = \mathbf{0}$; \mathbf{m}_t and \mathbf{v}_t are $d \times 1$ vectors containing exponential moving averages of the gradient and the squared gradient at iteration t , respectively; $\beta_1 \in [0, 1]$ and $\beta_2 \in [0, 1]$ are forgetting factors for the gradient and the squared gradient, respectively; $\eta > 0$ is a step size called the learning rate; and square, square root, division, and maximum operations are applied to vectors element-wise. When mini-batches are sampled uniformly at random with replacement and the learning rate is sufficiently small, AMSGrad is guaranteed to converge to a local stationary point for smooth, non-convex objective functions. Zhou, Tang, Yang, Cao, and Gu (2018) as well as Che, Liu, Sun, and Hong (2019) provide conditions required for first-order convergence, while Staib, Reddi, Kale, Kumar, and Sra (2019) discuss second-order convergence. Importantly, computation time per iteration does not increase with the sample size, allowing for convergence even

with very large-scale data (Bottou, Curtis, & Nocedal, 2018).

When ξ_t are FNN parameters, an algorithm called backpropagation (BP) is used to efficiently compute the gradient estimator in equation 5. BP is an application of the chain rule of calculus and is a special case of reverse mode automatic differentiation (Linnainmaa, 1970). Goodfellow, Bengio, and Courville (2016) provide a detailed discussion of BP.

3. The Problem of Fitting High-Dimensional Item Factor Analysis Models

3.1. The Graded Item Response Model

Samejima's (1969) graded response model (GRM) is a widespread model for polytomous item responses. We introduce notation for the GRM following Cai (2010a). Suppose there are $i = 1, \dots, N$ distinct respondents and $j = 1, \dots, J$ items. Let $y_{i,j} \in \{0, 1, \dots, C_j - 1\}$ denote the response for respondent i to item j in C_j graded (i.e., ordinal) categories. Note that when $C_j = 2$ for all j , the GRM reduces to the M2PL (McKinley & Reckase, 1983).

Suppose we have P LVs; let \mathbf{x}_i denote the $P \times 1$ vector of factor scores (i.e., LV values) for respondent i . Let β_j denote the $P \times 1$ vector of loadings, let $\alpha_j = (\alpha_{j1}, \dots, \alpha_{j,C_j-1})^\top$ denote the $(C_j - 1) \times 1$ vector of strictly ordered category intercepts, and let $\theta_j = (\alpha_j^\top, \beta_j^\top)^\top$ be a vector collecting all parameters for item j . The GRM defines a set of boundary response probabilities conditional on the item parameters θ_j and the factor scores \mathbf{x}_i :

$$\Pr(y_{i,j} \geq k \mid \theta_j, \mathbf{x}_i) = \frac{1}{1 + \exp[-D(\alpha_{j,k} + \beta_j^\top \mathbf{x}_i)]}, \quad k \in \{1, \dots, C_j - 1\}, \quad (8)$$

where $\Pr(y_{i,j} \geq 0 \mid \theta_j, \mathbf{x}_i) = 1$, $\Pr(y_{i,j} \geq C_j \mid \theta_j, \mathbf{x}_i) = 0$, and D is a scaling constant (typically 1.702) used to help the logistic metric better approximate the normal ogive metric (Reckase, 2009). The conditional probability for a particular response $y_{i,j} = k$,

$k \in \{0, \dots, C_j - 1\}$ is

$$\pi_{i,j,k} = P(y_{i,j} = k \mid \boldsymbol{\theta}_j, \mathbf{x}_i) = \Pr(y_{i,j} \geq k \mid \boldsymbol{\theta}_j, \mathbf{x}_i) - \Pr(y_{i,j} \geq k + 1 \mid \boldsymbol{\theta}_j, \mathbf{x}_i). \quad (9)$$

3.2. Observed Data Likelihood

It follows from equation 9 that the conditional distribution of $y_{i,j}$ is multinomial with C_j cells, trial size 1, and cell probabilities $\pi_{i,j,k}$:

$$p_{\boldsymbol{\theta}_j}(y_{i,j} \mid \mathbf{x}_i) = \prod_{k=0}^{C_j-1} \pi_{i,j,k}^{\mathbb{1}_k(y_{i,j})}, \quad (10)$$

where we define the indicator function

$$\mathbb{1}_k(y) = \begin{cases} 1, & \text{if } y = k \\ 0, & \text{otherwise} \end{cases} \quad (11)$$

for $k \in \{0, \dots, C_j - 1\}$. Let $\mathbf{y}_i = (y_{i,1}, \dots, y_{i,n})^\top$ be respondent i 's response pattern. By the usual conditional independence assumption, the conditional distribution of \mathbf{y}_i is

$$p_{\boldsymbol{\theta}}(\mathbf{y}_i \mid \mathbf{x}_i) = \prod_{j=1}^J p_{\boldsymbol{\theta}_j}(y_{i,j} \mid \mathbf{x}_i), \quad (12)$$

where $\boldsymbol{\theta}$ is a vector collecting the estimable parameters for all J items.

Assume the prior distribution of factor scores \mathbf{x}_i is standard multivariate normal with density function $\mathcal{N}(\mathbf{x}_i)$. Then the marginal distribution of \mathbf{y}_i is given by

$$p_{\boldsymbol{\theta}}(\mathbf{y}_i) = \int \prod_{j=1}^J p_{\boldsymbol{\theta}_j}(y_{i,j} \mid \mathbf{x}) \mathcal{N}(\mathbf{x}) d\mathbf{x}, \quad (13)$$

where the above integral is over \mathbb{R}^p . Let \mathbf{Y} be an $N \times J$ matrix of independent response

patterns whose i^{th} row is \mathbf{y}_i^\top . The observed data likelihood is

$$\mathcal{L}(\boldsymbol{\theta} \mid \mathbf{Y}) = \prod_{i=1}^N \left[\int \prod_{j=1}^J p_{\boldsymbol{\theta}_j}(y_{i,j} \mid \mathbf{x}) \mathcal{N}(\mathbf{x}) d\mathbf{x} \right]. \quad (14)$$

Maximizing $\mathcal{L}(\boldsymbol{\theta} \mid \mathbf{Y})$ directly is difficult because we must approximate the N integrals over \mathbb{R}^p numerically. In this work, we avoid this difficulty by deriving an analytical lower bound on $\log \mathcal{L}(\boldsymbol{\theta} \mid \mathbf{Y})$ using VI. We then maximize this lower bound using a DL algorithm.

4. Variational Methods for Item Factor Analysis

Variational inference (VI) is an approach to approximate maximum likelihood estimation for LV models that has recently gained traction in the machine learning community (Blei, Kucukelbir, & McAuliffe, 2017; Zhang, Butepage, Kjellstrom, & Mandt, 2019). VI has been applied for confirmatory IFA in both the frequentist setting (Curi et al., 2019) and the Bayesian setting (Chen, Filho, Prudncio, Diethe, & Flach, 2019; Natesan, Nandakumar, Minka, & Rubright, 2016; Wu et al., 2020) as well as for exploratory IFA in the frequentist setting (Hui, Warton, Ormerod, Haapaniemi, & Taskinen, 2017). In this section, we describe variational methods for IFA as well as an importance sampling technique for helping the variational estimator better approximate the MML estimator.

4.1. Variational Inference

We now describe VI in the context of a general LV model, then apply VI to IFA in the following sections. The main idea behind VI is to treat LV inference as an optimization problem. More formally, let $\mathbf{y} \in \mathcal{Y}$ and $\mathbf{x} \in \mathcal{X}$ denote observed and LVs, respectively, where \mathcal{Y} and \mathcal{X} are sample spaces. VI introduces a family \mathcal{Q} of approximate densities over LVs and aims to find the member $q_{\psi^*(\mathbf{y})}^*(\mathbf{x}) \in \mathcal{Q}$ that minimizes the Kullback-Leibler (KL)

divergence¹ from itself to the true LV posterior:

$$q_{\psi^*(\mathbf{y})}^*(\mathbf{x}) = \arg \min_{q_{\psi(\mathbf{y})}(\mathbf{x}) \in \mathcal{Q}} D_{\text{KL}} [q_{\psi(\mathbf{y})}(\mathbf{x}) \| p(\mathbf{x} | \mathbf{y})], \quad (15)$$

where $\psi(\mathbf{y})$ is a vector of variational parameters. Note that $\psi(\mathbf{y})$ depends on \mathbf{y} , indicating that a different vector of variational parameters is estimated for each observation. For models with continuous LVs, an often tractable choice for the approximate posterior is the isotropic normal density (Kingma & Welling, 2014):

$$q_{\psi(\mathbf{y})}(\mathbf{x}) = \mathcal{N}(\mathbf{x} | \boldsymbol{\mu}(\mathbf{y}), \boldsymbol{\sigma}^2(\mathbf{y})\mathbf{I}_P), \quad (16)$$

where $\boldsymbol{\mu}(\mathbf{y})$ is a $P \times 1$ vector of means, $\boldsymbol{\sigma}^2(\mathbf{y})$ is a $P \times 1$ vector of variances, and \mathbf{I}_P is a $P \times P$ identity matrix. Minimizing the KL divergence from the isotropic normal approximate posterior to the true LV posterior produces the “best” isotropic normal approximation to the true LV posterior. In practice, however, tractable approximate posteriors such as the isotropic normal density are rarely flexible enough to perfectly approximate the true LV posterior and thereby minimize the KL divergence to zero. The importance sampling technique described later in the section improves the accuracy of VI by implicitly increasing the flexibility of the approximate posterior.

4.2. Evidence Lower Bound

The log-likelihood of the observed data under the GRM can be written as a sum over the marginal likelihood of each observation:

$$\ell(\boldsymbol{\theta} | \mathbf{Y}) = \sum_{i=1}^N \log p_{\boldsymbol{\theta}}(\mathbf{y}_i), \quad (17)$$

¹For distributions q and p , the KL divergence is defined as $D_{\text{KL}} [q \| p] = \mathbb{E}_q [\log q] - \mathbb{E}_q [\log p]$. It can be shown that $D_{\text{KL}} [q \| p] \geq 0$ with equality if and only if $p = q$ almost everywhere w.r.t. q .

where $\ell(\boldsymbol{\theta} \mid \mathbf{Y}) = \log \mathcal{L}(\boldsymbol{\theta} \mid \mathbf{Y})$. Let the approximate LV posterior be the isotropic normal density as in equation 16. We can re-write a single summand in equation 17 as

$$\log p_{\boldsymbol{\theta}}(\mathbf{y}_i) = D_{\text{KL}} [q_{\boldsymbol{\psi}(\mathbf{y}_i)}(\mathbf{x}_i) \| p_{\boldsymbol{\theta}}(\mathbf{x}_i \mid \mathbf{y}_i)] + \mathbb{E}_{q_{\boldsymbol{\psi}(\mathbf{y}_i)}(\mathbf{x}_i)} [\log p_{\boldsymbol{\theta}}(\mathbf{x}_i, \mathbf{y}_i) - \log q_{\boldsymbol{\psi}(\mathbf{y}_i)}(\mathbf{x}_i)]. \quad (18)$$

The first term on the r.h.s. of equation 18 is the KL divergence from the approximate to the true LV posterior (i.e., it is the term we wish to minimize from equation 15). Since this term is non-negative, the second term on the r.h.s. of equation 18 is a lower bound on the marginal likelihood of a single observation. This term is called the evidence lower bound (ELBO) and can be re-written as

$$\log p_{\boldsymbol{\theta}}(\mathbf{y}_i) \geq \mathbb{E}_{q_{\boldsymbol{\psi}(\mathbf{y}_i)}(\mathbf{x}_i)} [\log p_{\boldsymbol{\theta}}(\mathbf{x}_i, \mathbf{y}_i) - \log q_{\boldsymbol{\psi}(\mathbf{y}_i)}(\mathbf{x}_i)] \quad (19)$$

$$= \mathbb{E}_{q_{\boldsymbol{\psi}(\mathbf{y}_i)}(\mathbf{x}_i)} [\log p_{\boldsymbol{\theta}}(\mathbf{y}_i \mid \mathbf{x}_i)] - D_{\text{KL}} [q_{\boldsymbol{\psi}(\mathbf{y}_i)}(\mathbf{x}_i) \| p_{\boldsymbol{\theta}}(\mathbf{x}_i)] \quad (20)$$

$$= \text{ELBO}_i. \quad (21)$$

The first term in the ELBO on line 20 is an expected conditional log-likelihood that encourages $q^*(\mathbf{x}_i \mid \mathbf{y}_i)$ to place mass on LVs that explain the observed data well, while the second term encourages densities that are close to the LV prior $p_{\boldsymbol{\theta}}(\mathbf{x}_i)$. Maximizing the ELBO over all observations w.r.t. the item parameters $\boldsymbol{\theta}$ and the variational parameters $\boldsymbol{\psi}(\mathbf{y}_i)$ both approximately maximizes the observed data log-likelihood and minimizes the KL divergence from the approximate to the true LV posterior.

4.3. Amortized Variational Inference

Traditional VI fits a different approximate LV posterior for each observation, which quickly becomes computationally infeasible for large data sets. It is also not straightforward to apply models fitted using VI to previously unseen observations (e.g., to perform LV inference for or to compute the log-likelihood of the unseen observations).

Amortized variational inference (AVI) is a computationally efficient alternative to VI that uses a powerful function approximator called an inference model to parameterize the approximate posterior. By sharing the parameters of the inference model across observations, AVI estimates a constant number of parameters regardless of the sample size, whereas VI estimates a number of parameters that at best grows linearly as a function of the sample size. Further, models fitted using AVI can easily be applied to previously unseen observations by simply feeding the observations to the inference model.

The variational autoencoder (VAE; Kingma & Welling, 2014; Rezende, Mohamed, & Wierstra, 2014) is an AVI algorithm whose inference model is an ANN. We can use a VAE for IFA by parameterizing the approximate LV posterior as follows:

$$\begin{aligned} (\boldsymbol{\mu}_i^\top, \log \boldsymbol{\sigma}_i^\top)^\top &= \text{FNN}_\phi(\mathbf{y}_i), \\ q_\phi(\mathbf{x}_i \mid \mathbf{y}_i) &= \mathcal{N}(\mathbf{x}_i \mid \boldsymbol{\mu}_i, \boldsymbol{\sigma}_i^2 \mathbf{I}_P), \end{aligned} \tag{22}$$

where $\boldsymbol{\mu}_i$ is a $P \times 1$ predicted vector of means, $\log \boldsymbol{\sigma}_i$ is a $P \times 1$ predicted vector of log-standard deviations, and FNN_ϕ is an L -layer FNN parameterized by ϕ . Rather than estimating a set of variational parameters $\boldsymbol{\psi}(\mathbf{y}_i)$ for each observation, the FNN parameters ϕ are now shared across observations. That is, rather than maximizing equation 20 over observations, we now maximize

$$\text{ELBO}_i = \mathbb{E}_{q_\phi(\mathbf{x}_i \mid \mathbf{y}_i)} [\log p_\theta(\mathbf{y}_i \mid \mathbf{x}_i)] - D_{\text{KL}} [q_\phi(\mathbf{x}_i \mid \mathbf{y}_i) \parallel p_\theta(\mathbf{x}_i)] \tag{23}$$

over observations. In theory, the VAE is equivalent to VI when the FNN is sufficiently flexible (e.g., when the FNN has one infinitely large hidden layer). In practice, the FNN has finite capacity and may prevent the VAE from performing as well as VI. This performance difference is called the amortization gap and may be reduced by increasing the flexibility of the approximate LV posterior (Cremer, Li, & Duvenaud, 2018).

4.4. Fitting the Amortized Model

Fitting the VAE for IFA can be accomplished with AMSGrad and BP after obtaining an unbiased estimator for the gradient of the ELBO w.r.t. the model parameters $\boldsymbol{\theta}$ and $\boldsymbol{\phi}$. An unbiased estimator for the gradient of the ELBO w.r.t. the item parameters $\boldsymbol{\theta}$ is

$$\nabla_{\boldsymbol{\theta}} \text{ELBO}_i = \nabla_{\boldsymbol{\theta}} \mathbb{E}_{q_{\boldsymbol{\phi}}(\mathbf{x}_i | \mathbf{y}_i)} [\log p_{\boldsymbol{\theta}}(\mathbf{x}_i, \mathbf{y}_i) - \log q_{\boldsymbol{\phi}}(\mathbf{x}_i | \mathbf{y}_i)] \quad (24)$$

$$= \mathbb{E}_{q_{\boldsymbol{\phi}}(\mathbf{x}_i | \mathbf{y}_i)} [\nabla_{\boldsymbol{\theta}} \log p_{\boldsymbol{\theta}}(\mathbf{x}_i, \mathbf{y}_i)] \quad (25)$$

$$\approx \frac{1}{S} \sum_{s=1}^S \nabla_{\boldsymbol{\theta}} \log p_{\boldsymbol{\theta}}(\mathbf{y}_i, \mathbf{x}_{i,s}), \quad (26)$$

where line 26 approximates the expectations in line 25 with a size S Monte Carlo sample of factor scores from the approximate LV posterior.² Obtaining an unbiased estimator for the gradient of the ELBO w.r.t. the FNN parameters $\boldsymbol{\phi}$ is more challenging because, in general,

$$\nabla_{\boldsymbol{\phi}} \text{ELBO}_i = \nabla_{\boldsymbol{\phi}} \mathbb{E}_{q_{\boldsymbol{\phi}}(\mathbf{x}_i | \mathbf{y}_i)} [\log p_{\boldsymbol{\theta}}(\mathbf{x}_i, \mathbf{y}_i) - \log q_{\boldsymbol{\phi}}(\mathbf{x}_i | \mathbf{y}_i)] \quad (27)$$

$$\neq \mathbb{E}_{q_{\boldsymbol{\phi}}(\mathbf{x}_i | \mathbf{y}_i)} [\nabla_{\boldsymbol{\phi}} \log p_{\boldsymbol{\theta}}(\mathbf{x}_i, \mathbf{y}_i) - \nabla_{\boldsymbol{\phi}} \log q_{\boldsymbol{\phi}}(\mathbf{x}_i | \mathbf{y}_i)], \quad (28)$$

since the expectations are taken w.r.t. $q_{\boldsymbol{\phi}}(\mathbf{x}_{i,s} | \mathbf{y}_i)$, which is a function of $\boldsymbol{\phi}$. To overcome this problem, we reparameterize \mathbf{x}_i as follows:

$$\begin{aligned} \boldsymbol{\epsilon}_i &\sim \mathcal{N}(\boldsymbol{\epsilon}_i), \\ \mathbf{x}_i &= \boldsymbol{\mu}_i + \boldsymbol{\sigma}_i \odot \boldsymbol{\epsilon}_i, \end{aligned} \quad (29)$$

where $\boldsymbol{\epsilon}_i$ is a $P \times 1$ sample from a standard multivariate normal density for observation i , $\boldsymbol{\mu}_i$ and $\boldsymbol{\sigma}_i$ are the outputs of the FNN inference model given in equations 22, and \odot denotes element-wise multiplication. This reparameterization “externalizes” the

²We move the gradient inside the expectation in line 25 using the fact that $q_{\boldsymbol{\phi}}(\mathbf{x}_i | \mathbf{y}_i)$, $\log p_{\boldsymbol{\theta}}(\mathbf{x}_i, \mathbf{y}_i)$, and $\log q_{\boldsymbol{\phi}}(\mathbf{x}_i)$ satisfy certain regularity conditions. For details, see Lehmann and Casella (1998).

randomness in \mathbf{x}_i by writing \mathbf{x}_i as a deterministic function of ϕ . We can now obtain an unbiased estimator for the gradient of the ELBO w.r.t. ϕ as follows:

$$\nabla_{\phi} \text{ELBO}_i = \nabla_{\phi} \mathbb{E}_{\mathcal{N}(\epsilon_i)} [\log p_{\theta}(\mathbf{x}_i, \mathbf{y}_i) - \log q_{\phi}(\mathbf{x}_i | \mathbf{y}_i)] \quad (30)$$

$$= \mathbb{E}_{\mathcal{N}(\epsilon_i)} [\nabla_{\phi} \log p_{\theta}(\mathbf{x}_i, \mathbf{y}_i) - \nabla_{\phi} \log q_{\phi}(\mathbf{x}_i | \mathbf{y}_i)] \quad (31)$$

$$\approx \frac{1}{S} \sum_{s=1}^S [\nabla_{\phi} \log p_{\theta}(\mathbf{x}_{i,s}, \mathbf{y}_i) - \nabla_{\phi} \log q_{\phi}(\mathbf{x}_{i,s} | \mathbf{y}_i)], \quad (32)$$

where the expectations are now taken w.r.t. $\mathcal{N}(\epsilon_i)$ and line 32 is a Monte Carlo approximation to the expectation in line 31. Figure 2 illustrates how computation proceeds in a VAE for IFA. We note that the KL divergence term shown has a closed form that is efficient to compute (Kingma & Welling, 2014):

$$D_{\text{KL}} [\mathcal{N}(\mathbf{x}_i | \boldsymbol{\mu}_i, \boldsymbol{\sigma}_i^2 \mathbf{I}_P) || \mathcal{N}(\mathbf{x}_i)] = \frac{1}{2} \sum_{p=1}^P [\mu_{i,p}^2 + \sigma_{i,p}^2 - 1 - \log \sigma_{i,p}^2]. \quad (33)$$

=====

Insert Figure 2 about here

=====

4.5. Importance-Weighted Variational Inference

Importance-weighted variational inference (IWVI; Burda, Grosse, & Salakhutdinov, 2016; Domke & Sheldon, 2018) is a VI strategy that can approximate the true log-likelihood arbitrarily well. Amortized IWVI for IFA maximizes a lower bound called

the importance-weighted ELBO (IW-ELBO):

$$\log p_{\boldsymbol{\theta}}(\mathbf{y}_i) \geq \text{IW-ELBO}_i \quad (34)$$

$$= \mathbb{E}_{q_{\boldsymbol{\phi}}(\mathbf{x}_{i,1}|\mathbf{y}_i) \cdots q_{\boldsymbol{\phi}}(\mathbf{x}_{i,R}|\mathbf{y}_i)} \left[\log \frac{1}{R} \sum_{r=1}^R \frac{p_{\boldsymbol{\theta}}(\mathbf{x}_{i,r}, \mathbf{y}_i)}{q_{\boldsymbol{\phi}}(\mathbf{x}_{i,r} | \mathbf{y}_i)} \right] \quad (35)$$

$$\approx \frac{1}{S} \sum_{s=1}^S \left[\log \frac{1}{R} \sum_{r=1}^R w_{i,r,s} \right] \quad (36)$$

where $w_{i,r,s} = p_{\boldsymbol{\theta}}(\mathbf{x}_{i,r,s}, \mathbf{y}_i) / q_{\boldsymbol{\phi}}(\mathbf{x}_{i,r,s} | \mathbf{y}_i)$ are unnormalized importance weights for the joint distribution of latent and observed variables, R is the number of importance samples, and line 36 is a Monte Carlo approximation to the expectation in line 35. When $R = 1$, the IW-ELBO reduces to the ELBO. As $R \rightarrow \infty$, the IW-ELBO converges monotonically to the marginal log-likelihood (Burda, Grosse, & Salakhutdinov, 2016) and the approximate LV posterior converges to the true LV posterior pointwise (Cremer, Morris, & Duvenaud, 2017). In other words, IWVI is equivalent to MML estimation when the number of importance samples R equals infinity, in which case IWVI inherits the MML estimator’s asymptotic properties. When $q_{\boldsymbol{\phi}}(\mathbf{x}_i | \mathbf{y}_i)$ is an FNN, the associated IWVI algorithm is called the importance-weighted autoencoder (Burda, Grosse, & Salakhutdinov, 2016).

Optimizing the IW-ELBO permits trading computational efficiency for a better approximation to the MML estimator by increasing R . A drawback of IWVI, however, is that increasing R can degrade performance of the gradient estimator for the inference model parameters $\boldsymbol{\phi}$. Specifically, Rainforth et al. (2018) theoretically and empirically show that as R increases, the signal-to-noise ratio of the inference model gradient estimator tends to zero so that the estimator becomes completely random. This problem can be mitigated, however, by increasing the number of samples S used for Monte Carlo approximation of the IW-ELBO or the number of mini-batch samples M used for our AMSGrad optimization procedure (Rainforth et al., 2018). We find this simple solution performs reasonably for our purposes, although we note that other solutions are available

(e.g., Tucker, Lawson, Gu, & Maddison, 2019).

5. Implementation Details

5.1. Starting Values

The proposed algorithm is detailed in Algorithm 1. We now discuss choosing the algorithm starting values $\boldsymbol{\xi}_0 = (\boldsymbol{\theta}_0^\top, \boldsymbol{\phi}_0^\top)^\top$.

=====
 Insert Algorithm 1 about here
 =====

The inference model starting values $\boldsymbol{\phi}_0$ include a $P_l \times P_{l-1}$ regression weight matrix $\mathbf{W}_0^{(l)}$ and a $P_l \times 1$ intercept vector $\mathbf{b}_0^{(l)}$ at FNN layers $l = 1, \dots, L$. We initialize these parameters using a variant of Kaiming initialization (He et al., 2015), which has demonstrated good performance when applied to ANNs with asymmetric activation functions (e.g., the ELU function). Let $\mathcal{U}(a, b)$ denote a uniform density with lower bound a and upper bound b . We randomly sample starting values as

$$w_{p_1, p_{l-1}, 0}^{(l)}, b_{p_l, 0}^{(l)} \sim \mathcal{U}\left(-\frac{1}{\sqrt{P_{l-1}}}, \frac{1}{\sqrt{P_{l-1}}}\right) \quad (37)$$

for $p_l = 1, \dots, P_l$, $p_{l-1} = 1, \dots, P_{l-1}$, $l = 1, \dots, L$. This initialization strategy often prevents the FNN hidden layer values from growing too large or too small at the start of fitting while accounting for the asymmetry of the ELU activation function around zero.

The starting values $\boldsymbol{\theta}_0$ include the $P \times 1$ factor loadings vector $\boldsymbol{\beta}_{j,0}$ as well as the $(C_j - 1) \times 1$ intercept vector $\boldsymbol{\alpha}_{j,0}$ for items $j = 1, \dots, J$. We initialize the factor loadings using Xavier initialization (Glorot & Bengio, 2010), which performs well when applied to

ANNs with symmetric activation functions:

$$\beta_{j,p,0}^{(l)} \sim \mathcal{U}\left(-\sqrt{\frac{6}{J+P}}, \sqrt{\frac{6}{J+P}}\right), \quad (38)$$

where $j = 1, \dots, J$ and $p = 1, \dots, P$. This approach stabilizes fitting in a manner similar to Kaiming initialization while accounting for the symmetry of the inverse logistic link function (i.e., equation 8) around zero. For $j = 1, \dots, J$, we initialize the elements of $\boldsymbol{\alpha}_{j,0}$ to an increasing sequence such that the cumulative density of logistic distribution between consecutive elements is the same (Christensen, 2019).

5.2. Stabilizing Fitting and Checking Convergence

We use a KL annealing strategy to avoid entrapment in local optima at the start of fitting (Bowman et al., 2016; Snderby et al., 2016). KL annealing multiplies the KL divergence term by t/τ for the first τ fitting iterations where $t = 0, \dots, \tau - 1$. We conduct KL annealing for $\tau = 1000$ fitting iterations for all models.

Once KL annealing is completed, we determine convergence following Cremer, Li, and Duvenaud (2018). At each fitting iteration, we store the IW-ELBO computed for the associated mini-batch. After every 100 fitting iterations, we compute the average of the previous 100 mini-batch IW-ELBOs and compare this average to the previous best achieved average. If the best achieved average IW-ELBO does not improve after 10 such comparisons, fitting is terminated.

It is sometimes necessary to assess whether different optimization runs have converged to equivalent stationary points. We conduct these checks using the estimated loadings matrices. We compare loadings matrices across runs by first rotating the factor solution using the Geomin oblique rotation method (Yates, 1988). Next, we invert factors if the sum of their loadings is negative (Asparouhov & Muthn, 2009). We then select a reference matrix and find the column permutation of each comparison matrix that minimizes the

element-wise mean squared error (MSE). Finally, we compute Tucker’s congruence coefficient between the permuted matrices (Lorenzo-Seva & ten Berge, 2006). Solutions with congruence coefficients larger than 0.98 are deemed equivalent (MacCallum, Widaman, Zhang, & Hong, 1999). We note that to compare factor correlation solutions, the same inversion and permutation procedure is applied to both columns and rows of the estimated factor correlation matrices.

5.3. *Tuning Hyperparameters*

Inference model hyperparameters include the number and size of the FNN hidden layers. After some experimentation, we found that performance was relatively insensitive to these values. We therefore use a single hidden layer for all models and set the hidden layer size to a value close to the mean of the input layer size and twice the latent dimension P . This choice is based on the observation that “the optimal size of the hidden layer is usually between the size of the input and size of the output layers” (Heaton, 2008).

Optimization hyperparameters include the learning rate η ; the forgetting factors for the gradient and squared gradient, β_1 and β_2 ; and the mini-batch size M . We set $\eta = 0.01$ for most models. For some models with many factors and many items, the IW-ELBO diverged, so we set $\eta = 0.005$. This approach is based on Bengio’s (2012) observations that $\eta = 0.01$ performs well in practice and that η should be reduced if the objective function diverges. We set $\beta_1 = 0.9$ and $\beta_2 = 0.999$, which are default values typically recommended in practice (Reddi, Kale, & Kumar, 2018). Bengio (2012) notes that the mini-batch size M mostly impacts time to convergence rather than model performance, while Goodfellow, Bengio, and Courville (2016) note that setting M to a power of 2 typically reduces fitting times by facilitating GPU (or CPU) memory allocation. We therefore set $M = 128$ as a default value for all analyses.

Setting the number of importance-weighted samples R and the number of Monte Carlo samples S typically does not require extensive tuning but does require some consideration.

Increasing R improves the model’s approximation to the true marginal log-likelihood, while increasing S decreases the variance of the gradient estimates \mathbf{g}_t . However, computational complexity at each fitting iteration grows with rate $\mathcal{O}(RS)$. One reasonable approach taken by Rainforth et al. (2019) is to choose some fixed RS that converges in a reasonable amount of time (e.g., $RS = 12$) and to fit a few (R, S) pairs that are factors of the chosen product (e.g., $(R, S) \in \{(4, 3), (6, 2)\}$). Our experiments suggest that choosing small values for R and S works well in practice, since increasing R and S too much quickly incurs high computational cost.

The main hyperparameter that requires tuning is the latent dimension P . We tried tuning P using a pseudo-likelihood Bayesian information criterion (pseudo-BIC; Erosheva, Fienberg, & Joutard, 2007) as well as using a more computationally intensive 5-fold cross-validation (CV) approach (details available upon request) but found that both approaches performed poorly as N increased. We therefore use a more subjective scree plot approach based on the Monte Carlo CV method described by Hui, Warton, Ormerod, Haapaniemi, and Taskinen (2017). To construct each scree plot, we first create a holdout set by randomly sampling some percentage of the item responses without replacement. Let Ω denote the index set for the item responses in the holdout set and let Ω' denote the indices of the item responses excluding the holdout set. For a fixed P , we fit the model using the item responses indexed by Ω' . We denote the fitted parameters so obtained as $\hat{\boldsymbol{\theta}}$ and $\hat{\boldsymbol{\phi}}$. Treating the IW-ELBO with $R = 5000$ importance-weighted samples as a close approximation to the true log-likelihood (Cremer, Li, & Duvenaud, 2018), we predict the approximate log-likelihood for the holdout set as

$$\tilde{\ell}(P) = \sum_{i \in \Omega} \left[\log \frac{1}{5000} \sum_{r=1}^{5000} \frac{p_{\hat{\boldsymbol{\theta}}}(\mathbf{x}_{i,r}, \mathbf{y}_i)}{q_{\hat{\boldsymbol{\phi}}}(\mathbf{x}_{i,r} \mid \mathbf{y}_i)} \right]. \quad (39)$$

After performing the above procedure for several successive values of P , the scree plot is constructed by plotting $-\tilde{\ell}(P)$ against increasing P . The latent dimension coinciding with

an “elbow” in the plot may be selected. We note that this approach differs from traditional scree plots in that we plot predicted approximate log-likelihoods rather than eigenvalues, although both approaches are interpreted similarly (i.e., look for the “elbow”). We empirically evaluate this approach in the following section.

6. Numerical Illustrations

We now explore the proposed algorithm via numerical examples. Models were programmed with the machine learning library PyTorch (Version 1.1.6; Paszke et al., 2017) and were fitted on a laptop computer with a 2.8 GHz Intel Core i7 CPU and 16 GB of RAM (unless otherwise specified). Although GPU computing is directly supported in PyTorch and often speeds up fitting, we opted for CPU computing to enable fairer comparisons with other methods and to assess performance using hardware more typically available for psychology and education research.

6.1. Application to a Big-Five Personality Questionnaire

We first illustrate the proposed algorithm using 1,015,342 responses to Goldberg’s (1992) 50 Big-Five Factor Marker (FFM) items from the International Personality Item Pool (IPIP; Goldberg et al., 2006) downloaded from the Open-Source Psychometrics Project (<https://openpsychometrics.org/>). The IPIP-FFM items were designed to assess respondents’ levels of five personality factors: *Conscientiousness*, *openness*, *emotional stability*, *agreeableness*, and *extraversion*. Empirical Big-Five studies often yield substantial factor inter-correlations (e.g., Biesanz & West, 2004), so we permitted correlated factors by applying the Geomin oblique rotation method to all fitted loadings matrices. Each of the five factors included 10 five-category items anchored by “Disagree” (1), “Neutral” (3), and “Agree” (5). Item responses were recoded as necessary so that the highest numerical value of the response scale indicated a high level of the corresponding factor. After pre-processing the data (details available upon request), our final sample size was $N = 515,708$ responses.

Computation was carried out following the procedures described in Section 5. A scree plot of $-\tilde{\ell}(P)$ computed on a holdout set of 2.5% of observations for $P \in \{1, \dots, 10\}$ (Figure 3) demonstrated an “elbow” at $P = 5$, suggesting that 5 latent factors accounted for most of the correlation between item responses. We set the inference model hidden layer size to 130 (i.e., the mean of the input layer size and $2P$) and the learning rate to $\eta = 0.01$. Manual experimentation suggested that model performance was fairly insensitive to increasing the number of importance-weighted samples R and the number of Monte Carlo samples S . We therefore chose the smallest $R, S > 1$ to demonstrate the importance-weighting approach – that is, we set $R, S = 2$. We fitted the full data set 100 times to assess the replicability of the parameter estimates across random seeds. Only equivalent factor solutions were compared.

=====

Insert Figure 3 about here

=====

We report results from the fitted model that attained the highest IW-ELBO. Figure 4 contains a heatmap of the Geomin-rotated factor loadings estimates, which fit with the expected five factor structure. Factor correlations in Table 1 also fit with the typical finding that emotional stability is negatively correlated with the other factors. Notably, fitting was fast: Mean fitting time across random seeds was 124 seconds ($SD = 47$ seconds). Further, parameter estimates were fairly stable: Across random seeds, mean loadings root-mean-square error (RMSE) was 0.016 ($SD = 0.005$), mean intercepts RMSE was 0.058 ($SD = 0.028$), and mean factor correlation RMSE was 0.051 ($SD = 0.016$).

=====

Insert Figure 4 about here

=====

=====

Insert Table 1 about here

=====

6.2. Simulation Studies

6.2.1. Asymptotic Evaluation of the Variational Estimator

In this study, we assess the asymptotic properties of the amortized importance-weighted variational estimator as the number importance-weighted samples R increases (i.e., as the approximation to the marginal likelihood improves). We first fix the number of Monte Carlo samples $S = 8$ to reduce the variance of the gradient estimates. We then consider $R = 1, 8$, and 16 . The first setting uses the ELBO objective, while the latter settings use the IW-ELBO objective. Data generating loadings, intercepts, and factor correlations are rounded estimates from the IPIP-FFM example in section 6.1. We set $P = 5$, $J = 50$, and $C_j = 5$ for $j = 1, \dots, J$. Each factor loads on ten items with cross loadings set to zero to produce a perfect simple structure. To investigate the estimator’s properties in the classical asymptotic setting where $N \rightarrow \infty$, we conduct 100 replications of simulation for $N = 500, 1000, 2000$, and $10\,000$. This leads to 12 different simulation settings for all possible combinations of R and N . We also assessed the model selection performance of the scree plot approach by plotting $-\tilde{\ell}(P)$ computed on a holdout set of 20% of observations for $P \in \{2, \dots, 8\}$ at each replication. All inference model and optimization hyperparameters from section 6.1 were reused for these analyses. Models were fitted in parallel on a compute cluster where each compute node had a 2.50 GHz Intel processor with 16 GB of RAM.

To assess estimator bias at each simulation setting, we computed bias for each parameter as the mean deviation of the estimated parameter from the data generating

parameter across replications:

$$\text{bias}(\hat{\xi}, \xi) = \frac{1}{100} \sum_{a=1}^{100} [\hat{\xi}^{(a)} - \xi], \quad (40)$$

where $\hat{\xi}^{(a)}$ is the estimated parameter at replication a and ξ is the data generating parameter. Figure 5 uses boxplots to summarize the parameter biases separately for the factor loadings, factor correlations, and intercepts. Factor loadings and intercepts estimates appear to be unbiased and become more accurate with increasing N . Factor correlation estimates become more accurate but exhibit some bias as N increases. Intercepts and factor correlation estimates become less accurate with increasing R . We also assessed estimator efficiency by computing MSE for each parameter (i.e., by squaring the summands in equation 40). Results are summarized using boxplots in Figure 6. For each R setting, parameter MSE quickly decreases toward zero with increasing N , suggesting that IWVI is consistent. Factor correlation MSE decreased but was more variable than for the other estimates. Increasing R seemed to have a negligible impact on asymptotic efficiency.

=====

Insert Figure 5 about here

=====

=====

Insert Figure 6 about here

=====

Figure 7 contains line plots of fitting times for each simulation setting across replications. Increasing R leads to a large increase in time to convergence. Interestingly, median fitting time actually decreases for fixed R as N increases. This result highlights the scalability of AMSGrad to arbitrarily large data sets. To assess factor score estimation

accuracy at each replication, we first obtained maximum *a posteriori* (MAP) factor score estimates by computing the approximate LV posterior mean $\boldsymbol{\mu}_i$ for each item response. After rotating the scores and applying the inversion and column permutation procedure used to compare loadings solutions, we computed the correlation between the true and estimated scores for each latent factor. Estimates were accurate: For fixed R , correlations ranged from 0.88 to 0.95 and tended to increase with increasing N . The scree plot approach to tuning the latent dimension P appeared to perform well across simulation settings. Figure 8 presents scree plots for simulation settings where $N = 10\,000$, which possess sharp “elbows” at $P = 5$. Plots for other N settings were nearly identical and are not shown.

=====

Insert Figure 7 about here

=====

=====

Insert Figure 8 about here

=====

6.2.2. Comparison to MH-RM in the Classical Asymptotic Regime

In this study, we compare the asymptotic efficiency of the amortized variational estimator to the efficiency of the MML estimator implemented via the MH-RM algorithm. We note that the stEM algorithm is somewhat faster than MH-RM (Zhang, Che, & Liu, 2020) and may therefore be a suitable alternative comparison method. However, given that MH-RM is relatively widely used and that stEM has only been implemented for the M2PL, we choose MH-RM for these analyses. MH-RM is implemented via the R package *mirt* (Version 1.32.1; Chalmers, 2012). Comparing the computational efficiency of the proposed approach and MH-RM is therefore fair in the sense that both *mirt* and Pytorch core functions are written in C++ and comparisons are conducted on the same computer.

We compare these methods in the high-dimensional setting where $P = 10$, $J = 100$, and $C_j = 5$ for $j = 1, \dots, J$. Data generating parameters are again rounded estimates from the IPIP-FFM example. We set the parameters for items 51-100 equal to the parameters for items 1-50. We construct the factor correlation matrix as a 10×10 block diagonal matrix with main-diagonal blocks equal to the rounded IPIP-FFM estimates and zeros elsewhere. Results of the previous simulation suggest that increasing the number of importance-weighted samples R provides moderate to negligible benefits to the variational estimator at high computational cost. We therefore set $R = 1$ for these analyses and set $M = 4$ to reduce variance in the gradient estimates. All other hyperparameters are set as in previous sections. MH-RM hyperparameters were set to the mirt package defaults. We conduct 100 replications of simulation for $N = 1000, 2000, 5000$, and $10\,000$.

Results are shown in Figures 9 and 10. Both methods clearly produce accurate estimates. AVI achieves comparable efficiency to MH-RM, although MH-RM is often slightly more accurate. This difference in accuracy may in part be due to MH-RM’s procedure for choosing starting values, which involves conducting several stochastic EM-type iterations and averaging the estimates so obtained. However, AVI is much faster than MH-RM. MH-RM’s median fitting time increases from 8 minutes for $N = 1000$ to 21 minutes for $N = 10\,000$, whereas AVI’s median fitting time stays around 80 seconds regardless of N .

6.2.3. Comparison to CJMLE in the Double Asymptotic Regime

We also compare the efficiency of the amortized variational estimator with the efficiency of CJMLE in the double asymptotic setting where N and J increase simultaneously. Results due to Chen, Li, and Zhang (2019) suggest that the MML estimator implemented via MH-RM performs poorly in the double asymptotic setting and that CJMLE attains much faster convergence via an alternating minimization algorithm. CJMLE is implemented in the R package mirtjml (Version 1.4; Zhang, Chen, & Li, 2019)

and has core functions written in C++. Although CJMLE computation may be parallelized, we compare methods using a single core to ensure fairness.

We again set $P = 10$ and consider $(N, J) = (2000, 100), (10\,000, 200), (50\,000, 300)$, and $(100\,000, 400)$. CJMLE is only implemented for the M2PL, so we set $C_j = 2$ for $j = 1, \dots, J$. Data generating item parameters are again set by repeating the IPIP-FFM item parameters. For example, when $J = 400$, we repeat the parameters for items 1-50 seven times to get the parameters for items 51-400. Since each item needs only a single intercept, we randomly select an intercept from the four fitted IPIP-FFM intercepts for each item. The factor correlation matrix from section 6.2.2 is reused. Hyperparameters are set similarly to those in section 6.2.2, except we set $\eta = 0.005$ for $(N, J) = (50\,000, 300)$ and $(100\,000, 400)$ because these models sometimes experienced numerical issues otherwise.

Results are presented in Figures 11 and 12. Unlike the MML estimator, AVI demonstrates consistency in the double asymptotic setting and has comparable efficiency with CJMLE. CJMLE estimates loadings inaccurately in the smallest (N, J) setting but is slightly more accurate than AVI in the highest setting. This slight difference may again be partly due to starting values, which CJMLE obtains using a fast SVD estimator that performs best in the double asymptotic setting. Factor correlation estimation efficiency is not reported because CJMLE treats the LVs as fixed effects. Importantly, AVI is always faster than CJMLE. AVI's median fitting time is 43 seconds when $(N, J) = (2000, 100)$ and increases to just over 3 minutes when $(N, J) = (100\,000, 400)$, whereas CJMLE's median fitting time increases from 73 seconds to over 43 minutes in the same settings. We note that CJMLE may achieve a significant speedup using parallel computing, although AVI may achieve a similar speedup using a GPU.

7. Extensions

7.1. Confirmatory Item Factor Analysis

Confirmatory IFA is useful when sufficient prior theory exists to posit a specific factor structure for the items. More precisely, the measurement design may be indicated by a pre-specified $J \times P$ matrix \mathbf{Q} with entries $q_{j,p} \in \{0, 1\}$ such that $q_{j,p} = 1$ if item j measures factor p (i.e., $\beta_{j,p}$ is freely estimated) and $q_{j,p} = 0$ otherwise (i.e., $\beta_{j,p}$ is set to zero). Anderson and Rubin (1957) provide sufficient conditions on \mathbf{Q} to ensure the model is identified. The deep learning algorithm discussed here may be used to conduct confirmatory IFA by ensuring that factor loadings are either freely estimated or set to zero as specified in \mathbf{Q} (Curi et al., 2020). In the confirmatory setting, it is also typically of interest to impose constraints on the factor covariance matrix Σ . Letting $\Sigma = \mathbf{L}\mathbf{L}^\top$ where \mathbf{L} is a lower triangular matrix, we can estimate \mathbf{L} using Pinheiro and Bates' (1996) unconstrained spherical parameterization, which is computationally efficient, uniquely defined, and allows for arbitrary zero constraints on the elements of Σ .

7.2. Regularized Exploratory Item Factor Analysis

Regularization has been proposed as a viable alternative to factor rotation for both exploratory linear factor analysis (e.g., Choi, Oehlert, & Zou, 2010; Hirose & Konishi, 2012; Hirose & Yamamoto, 2014) and exploratory IFA (Hui, Tanaka, & Warton, 2018; Sun, Chen, Liu, Ying, & Xin, 2016). Many regularization approaches automatically rotate the factors to produce a sparse loadings structure. The regularized, amortized, importance-weighted variational estimator is obtained by solving the optimization problem

$$\boldsymbol{\xi}^* = \arg \max_{\boldsymbol{\xi}} \left[\sum_{i=1}^N \text{IW-ELBO}_i - \mathcal{P}(\mathbf{B}) \right], \quad (41)$$

where \mathbf{B} is a $J \times P$ factor loadings matrix whose j^{th} row is β_j and \mathcal{P} is a penalty function that is potentially non-smooth and non-convex. This optimization problem may be solved using a proximal version of AMSGrad based on the ProxGen procedure developed by Yun, Lozano, and Yang (2020), which is guaranteed to converge to a local stationary point when mild conditions are satisfied.

7.3. Flexible Latent Density Estimation

Recent work by Monroe (2014) aims to relax the assumption that the LVs are multivariate normally distributed. An alternative approach developed recently in the deep learning literature is based on the concept of normalizing flows (NFs; Tabak & Turner, 2012; Tabak & Vanden-Eijnden, 2010). NFs apply a sequence of invertible mappings parameterized by ANNs that aims to transform a simple base density into an arbitrarily complicated density. Since the mappings are invertible, the transformed density can be explicitly evaluated via the change of variables formula. NFs scale well to high-dimensional spaces and may be used to increase the flexibility of AVI by building complicated latent prior or posterior distributions (e.g., Huang, Krueger, Lacoste, & Courville, 2018; Kingma et al., 2016; Rezende & Mohamed, 2015).

7.4. Nonlinear Factor Analysis

The full VAE may be viewed as a model for nonlinear factor analysis (Yalcin & Amemiya, 2001) of the form

$$\mathbf{y}_i = g(\mathbf{x}_i) + \boldsymbol{\varepsilon}_i, \quad (42)$$

for $i = 1, \dots, N$ where g is an arbitrary nonlinear function and $\boldsymbol{\varepsilon}_i$ is the i^{th} $J \times 1$ vector of errors. In the VAE, g is approximated using an ANN. This corresponds to approximating the inverse link function between observed and latent variables while keeping the latent density fixed (Wu et al., 2020). This approach is typically less interpretable than

approximating the latent density and fixing g , which provides equivalent model fit (e.g., Woods & Thissen, 2006).

8. Discussion

In this paper, we explored the suitability of an amortized variational inference algorithm for exploratory IFA. Numerical studies highlighted several benefits of the proposed approach. Analysis of a large-scale Big-Five personality factors data set yielded fast results that aligned with existing psychological theory across random starts. Our simulations suggested that, unlike other estimators, the amortized variational estimator has comparable statistical efficiency to state-of-the-art estimators in both the classical asymptotic setting where the number of observations increases and in the double asymptotic setting where the number of items and the number of observations simultaneously increase. The amortized variational estimator converges faster than existing estimators when optimized using the adaptive stochastic gradient algorithm AMSGrad, particularly with large-scale data. Factor score estimates were accurate and improved with increasing sample size. The sampling-based initialization procedures appeared to mitigate problems associated with convergence to local optima and performed comparably to the more computationally intensive approaches used by MH-RM and CJMLE.

Two practical considerations not discussed here are standard errors (SEs) and missing data. Hui, Warton, Ormerod, Haapaniemi, and Taskinen (2017) note that for the former, approximate SEs may be obtained by evaluating the observed information matrix at the estimates $\hat{\theta}$ obtained by maximizing the IW-ELBO. Since this matrix has a block diagonal structure, it may be block-wise inverted to produce the covariance matrix from which SEs can be calculated. We note that SEs will likely be quite small for the large-scale applications considered here. Mattei and Frellsen (2019) discuss a simple approach to handling missing-at-random data in amortized IWVI that can be easily applied to the models considered here.

The proposed approach has several limitations. The main practical difficulty we encountered was tuning the number of latent factors P . Although we tried tuning P using objective methods such as computing a pseudo-BIC and conducting 5-fold CV, these methods typically failed for large sample sizes, possibly due to log-likelihood approximation error exceeding sampling error. We therefore used subjective log-likelihood scree plots to tune P . Research is needed to develop objective criteria for selecting the latent dimension in large samples. In the meantime, the more subjective scree plot approach used here as well as approaches such as parallel analysis and retaining theoretically meaningful factors may serve as practical substitutes.

As noted by Hui, Warton, Ormerod, Haapaniemi, and Taskinen (2017), substantial theoretical work remains to be done to show that variational approximations produce consistent, asymptotically normal estimators and to obtain their rates of convergence. The importance sampling approach explored here provides a theoretical link between VI and MML estimation. Interestingly, however, our simulations suggested that obtaining a better approximation to the true marginal likelihood using importance sampling provides negligible practical benefits and may decrease intercept and factor correlation estimate accuracy. Additionally, factor correlation estimates exhibited some bias both with and without importance sampling. These results should be further explored in future work.

Notwithstanding these limitations, the present research suggests that amortized variational inference is a feasible and promising approach to high-dimensional exploratory IFA for psychological and educational measurement, performing well in both the single and double asymptotic settings and permitting quick, accurate exploration of large-scale data sets. Additionally, AVI has many other compelling benefits that are worthy of further exploration. The rapidly developing DL literature includes a huge number of extensions that could enhance modeling and estimation in a wide variety of contexts. We view AVI as part of a progression that started with the linear models of classical test theory, transitioned to the partially nonlinear models of IRT, and is now advancing to utilize the

fully nonlinear models available in machine learning. We hope our work will aid this progression by helping to spur a fruitful dialogue between the fields of machine learning and psychometrics.

References

- Anderson, T., & Rubin, H. (1957). Statistical inference in factor analysis. *Proceedings of the Third Berkeley Symposium on Mathematical Statistics and Probability*, 5, 111-150.
- Asparouhov, T., & Muthén, B. (2009). Exploratory structural equation modeling. *Structural Equation Modeling: A Multidisciplinary Journal*, 16 (3), 397-438.
- Bguin, A. A., & Glas, C. A. W. (2001). MCMC estimation and some model-fit analysis of multidimensional IRT models. *Psychometrika*, 66 (4), 541-562.
- Bengio, Y. (2012). Practical recommendations for gradient-based training of deep architectures. In *Neural Networks: Tricks of the Trade* (pp. 437-478). Springer, Berlin, Heidelberg.
- Biesanz, J. C., & West, S. G. (2004). Towards understanding assessments of the Big Five: Multitrait-multimethod analyses of convergent and discriminant validity across measurement occasion and type of observer. *Journal of Personality*, 72 (4), 845-876.
- Blei, D. M., Kucukelbir, A., & McAuliffe, J. D. (2017). Variational inference: A review for statisticians. *Journal of the American Statistical Association*, 112 (518), 859-877.
- Bock, R. D., & Aitkin, M. (1981). Marginal maximum likelihood estimation of item parameters: Application of an EM algorithm. *Psychometrika*, 46 (4), 443-459.
- Bock, R. D., Gibbons, R., & Muraki, E. (1988). Full-information item factor analysis. *Applied Psychological Measurement*, 12 (3), 261-280.
- Bolt, D. M. (2005). Limited- and full-information estimation of item response theory models. In A. Maydeau-Olivares & J. J. McArdle (Eds.), *Contemporary psychometrics* (Chap. 2, pp. 27-72). Mahwah, New Jersey: Lawrence Erlbaum Associates, Inc.
- Bottou, L., Curtis, F. E., & Nocedal, J. (2018). Optimization methods for large-scale machine learning. *SIAM Review*, 60 (2), 223-311.

- Bowman, S. R., Vilnis, L., Vinyals, O., Dai, A. M., Jozefowicz, R., & Bengio, S. (2016). Generating sentences from a continuous space. *Conference on Computational Natural Language Learning Proceedings*, 10-21.
- Burda, Y., Grosse, R. & Salakhutdinov, R. (2016). Importance weighted autoencoders. 4th International Conference on Learning Representations (ICLR 2016), 1-14.
- Cai, L. (2010a). High-dimensional exploratory item factor analysis by a Metropolis-Hastings Robbins-Monro algorithm. *Psychometrika*, 75 (1), 33-57.
- Cai, L. (2010b). Metropolis-Hastings Robbins-Monro algorithm for confirmatory item factor analysis. *Journal of Educational and Behavioral Statistics*, 35 (3), 307-335.
- Chalmers, R. P. (2012). Mirt: A multidimensional item response theory package for the R environment. *Journal of Statistical Software*, 48 (6), 1-29.
- Chen, Y., Filho, T. S., Prudncio, R. B. C., Diethe, T., & Flach, P. (2019). β^3 -IRT : A new item response model and its applications. *Proceedings of the 22nd International Conference on Artificial Intelligence and Statistics (AISTATS 2019)*, 89.
- Chen, Y., Li, X., & Zhang, S. (2019). Joint maximum likelihood estimation for high-dimensional exploratory item factor analysis. *Psychometrika*, 84 (1), 124-146.
- Chen, X., Liu, S., Sun, R., & Hong, M. (2019). On the convergence of a class of ADAM-type algorithms for non-convex optimization. *7th International Conference on Learning Representations (ICLR 2019)*.
- Choi, J., Oehlert, G., & Zou, H. (2010). A penalized maximum likelihood approach to sparse factor analysis. *Statistics and Its Interface*, 3 (4), 429-436.
- Christensen, R. H. B. (2019). Cumulative link models for ordinal regression with the R package ordinal. Submitted in *Journal of Statistical Software*. Retrieved from www.jstatsoft.org/

- Clevert, D. A., Unterthiner, T., & Hochreiter, S. (2016). Fast and accurate deep network learning by exponential linear units (ELUs). *4th International Conference on Learning Representations (ICLR 2016)*, 1-14.
- Cremer, C., Li, X., & Duvenaud, D. (2018). Inference suboptimality in variational autoencoders. *35th International Conference on Machine Learning (ICML 2018)*, 3, 1749-1760.
- Curi, M., Converse, G. A., Hajewski, J., & Oliveira, S. (2019). Interpretable Variational Autoencoders for Cognitive Models. In *2019 International Joint Conference on Neural Networks*. Retrieved from <https://ieeexplore.ieee.org/document/8852333>
- Cybenko, G. (1989). Approximation by superpositions of a sigmoidal function. *Mathematics of Control, Signals, and Systems*, 2, 303-314.
- Domke, J., & Sheldon, D. (2018). Importance weighting and variational inference. *Advances in Neural Information Processing Systems*, 4470-4479.
- Duchi, J. C., Hazan, E., Singer, Y. (2011). Adaptive subgradient methods for online learning and stochastic optimization. *Journal of Machine Learning Research*, 12, 2121-2159.
- Edwards, M. (2010). A Markov chain Monte Carlo approach to confirmatory item factor analysis. *Psychometrika*, 75 (3), 474-497.
- Erosheva, E. A., Fienberg, S. E., & Joutard, C. (2007). Describing disability through individual-level mixture models for multivariate binary data. *The Annals of Applied Statistics*, 1 (2), 502-537.
- Gershman, S., & Goodman, N. (2014). Amortized inference in probabilistic reasoning. *Proceedings of the 36th Annual Conference of the Cognitive Science Society (CogSci 2014)*, 1, 517-522.

- Glorot, X., & Bengio, Y. (2010). Understanding the difficulty of training deep feedforward neural networks. *Journal of Machine Learning Research*, 9, 249-256.
- Goldberg, L. R. (1992). The development of markers for the Big-Five factor structure. *Psychological Assessment*, 4 (1), 26-42.
- Goldberg, L. R., Johnson, J. A., Eber, H. W., Hogan, R., Ashton, M. C., Cloninger, C. R., & Gough, H. G. (2006). The international personality item pool and the future of public-domain personality measures. *Journal of Research in Personality*, 40 (1), 84-96.
- Goodfellow, I., Bengio, Y., & Courville, A. (2016). *Deep learning*. Cambridge, MA: MIT Press.
- He, K., Zhang, X., Ren, S., & Sun, J. (2015). Delving deep into rectifiers: Surpassing human-level performance on ImageNet classification. *Proceedings of the IEEE International Conference on Computer Vision*, 1026-1034.
- Heaton, J. (2008). *Introduction to Neural Networks for Java* (2nd ed.). Chesterfield, MO: Heaton Research, Inc.
- Hirose, K., & Konishi, S. (2012). Variable selection via the weighted group lasso for factor analysis models. *The Canadian Journal of Statistics*, 40 (2), 345-361.
- Huang, C. W., Krueger, D., Lacoste, A., & Courville, A. (2018). Neural autoregressive flows. *35th International Conference on Machine Learning (ICML 2018)*, 5, 3309-3324.
- Huber, P., Ronchetti, E., & Victoria-Feser, M.-P. (2004). Estimation of generalized linear latent variable models. *Journal of the Royal Statistical Society – Series B*, 66 (4), 893-908.
- Hui, F. K. C., Tanaka, E., & Warton, D. I. (2018). Order selection and sparsity in latent variable models via the ordered factor LASSO. *Biometrics*, 74 (4), 1311-1319.

- Hui, F. K. C., Warton, D. I., Ormerod, J. T., Haapaniemi, V., & Taskinen, S. (2017). Variational approximations for generalized linear latent variable models. *Journal of Computational and Graphical Statistics*, 26 (1), 35-43.
- Jordan, M. I., Ghahramani, Z., Jaakkola, T. S., & Saul, L. K. (1998). *Learning in Graphical Models*, 37, 183-233.
- Jreskog, K. G., & Moustaki, I. (2001). Factor analysis of ordinal variables: A comparison of three approaches. *Multivariate Behavioral Research*, 36 (3), 347-387.
- Kingma, D. P., Salimans, T., Jozefowicz, R., Chen, X., Sutskever, I., & Welling, M. (2016). Improved variational inference with inverse autoregressive flow. *Advances in Neural Information Processing Systems*, 4743-4751.
- Kingma, D. P., & Welling, M. (2014). Auto-encoding variational Bayes. *International Conference on Learning Representations*, 1-15.
- Lehmann, E. L., & Casella, G. (1998). *Theory of point estimation*. New York, NY: Springer-Verlag.
- Linnainmaa, S. (1970). The representation of the cumulative rounding error of an algorithm as a Taylor expansion of the local rounding errors. *Master's Thesis (in Finnish)*, University of Helsinki.
- Lorenzo-Seva, U., & ten Berge, J. M. (2006). Tuckers congruence coefficient as a meaningful index of factor similarity. *Methodology: European Journal of Research Methods for The Behavioral and Social Sciences*, 2 (2), 57-64.
- MacCallum, R. C., Widaman, K. F., Zhang, S., & Hong, S. (1999). Sample size in factor analysis. *Psychological Methods*, 4 (1), 84-99.
- Mattei, P.-A., & Frellsen, J. (2019). MIWAE: Deep generative modelling and imputation of incomplete data. *Proceedings of Machine Learning Research*, 97, 4413-4423.

- McKinley, R., & Reckase, M. (1983). *An extension of the two-parameter logistic model to the multidimensional latent space* (Research Report ONR83-2). Iowa City: The American College Testing Program.
- McMahan, H. B., & Streeter, M. (2010). Adaptive bound optimization for online convex optimization. *The 23rd Conference on Learning Theory (COLT 2010)*, 244-256.
- Meng, X.-L., & Schilling, S. (1996). Fitting full-information item factor models and an empirical investigation of bridge sampling. *Journal of the American Statistical Association*, 91 (435), 1254-1267.
- Monroe, S. L. (2014). Multidimensional item factor analysis with semi-nonparametric latent densities. Unpublished doctoral dissertation. Los Angeles, CA: University of California.
- Muthn, B. (1978). Contributions to factor analysis of dichotomous variables. *Psychometrika*, 43 (4), 551-560.
- Muthn, B. (1984). A general structural equation model with dichotomous, ordered categorical, and continuous latent variable indicators. *Psychometrika*, 49 (1), 115-132.
- Natesan, P., Nandakumar, R., Minka, T., & Rubright, J. D. (2016). Bayesian prior choice in IRT estimation using MCMC and variational Bayes. *Frontiers in Psychology*, 7, Article 1422.
- Nemirovski, A., Juditsky, A., Lan, G. & Shapiro, A. (2009). Robust stochastic approximation approach to stochastic programming. *SIAM Journal on Optimization*, 19 (4), 1574-1609.
- Paszke, A., Gross, S., Chintala, S., Chanan, G., Yang, E., DeVito, Z., . . . , Lerer, A. (2017). Automatic differentiation in PyTorch. *Workshop on Neural Information Processing Systems*.
- Pinheiro, J. C., & Bates, D. M. (1996). Unconstrained parametrizations for variance-covariance matrices. *Statistics and Computing*, 6 (3), 289-296.

- Rabe-Hesketh, S., Skrondal, A., & Pickles, A. (2005). Maximum likelihood estimation of limited and discrete dependent variable models with nested random effects. *Journal of Econometrics*, 128 (2), 301-323.
- Rainforth, T., Kosiorek, A. R., Le, T. A., Maddison, C. J., Igl, M., . . . , Teh, Y. W. (2018). Tighter variational bounds are not necessarily better. *35th International Conference on Machine Learning, (ICML 2018)*, 10, 6818-6832.
- Reckase, M. D. (2009). *Multidimensional item response theory*. Springer-Verlag.
- Reddi, S. J., Kale, S., & Kumar, S. (2018). On the convergence of ADAM and beyond. *International Conference on Learning Representations*.
- Rezende, D. J., Mohamed, S., & Wierstra, D. (2014). Stochastic backpropagation and approximate inference in deep generative models. *Proceedings of the 31st International Conference on Machine Learning*, 32 (2), 1278-1286.
- Rezende, D. J., & Mohamed, S. (2015). Variational inference with normalizing flows. *32nd International Conference on Machine Learning (ICML 2015)*, 2, 1530-1538.
- Robbins, H., & Monro, S. (1951). A stochastic approximation method. *The Annals of Mathematical Statistics*, 400-407.
- Samejima, F. (1969). Estimation of latent ability using a response pattern of graded scores. *Psychometrika*, 35 (1), 139.
- Schilling, R., & Bock, D. (2005). High-dimensional maximum marginal likelihood item factor analysis by adaptive quadrature. *Psychometrika*, 70 (3), 533-555.
- Snderby, C. K., Raiko, T., Maale, L., Snderby, S. K., & Winther, O. (2016). Ladder variational autoencoders. *Advances in Neural Information Processing Systems*, 3745-3753.
- Song, X., & Lee, S. (2005). A multivariate probit latent variable model for analyzing dichotomous responses. *Statistica Sinica*, 15 (3), 45-64.

- Spall, J. C. Introduction to stochastic search and optimization: estimation, simulation, and control. John Wiley & Sons, Inc.
- Staib, M., Reddi, S., Kale, S., Kumar, S., & Sra, S. (2019). Escaping saddle points with adaptive gradient methods. *36th International Conference on Machine Learning (ICML 2019)*, 10420-10454.
- Sun, J., Chen, Y., Liu, J., Ying, Z., & Xin, T. Latent variable selection for multidimensional item response theory models via L1 regularization. *Psychometrika*, 81 (4), 921-939.
- Tabak, E. G., & Turner, C. V. (2012). A family of nonparametric density estimation algorithms. *Communications on Pure and Applied Mathematics*, 66 (2), 145-164.
- Tabak, E. G., & Vanden-Eijnden, E. (2010). Density estimation by dual ascent of the log-likelihood. *Communications in Mathematical Sciences*, 8 (1), 217-233.
- Tucker, G., Maddison, C. J., Lawson, D., & Gu, S. (2019). Doubly reparameterized gradient estimators for Monte Carlo objectives. *7th International Conference on Learning Representations (ICLR 2019)*.
- van der Linden, D., te Nijenhuis, J., & Bakker, A. B. (2010). The General Factor of Personality: A meta-analysis of Big Five intercorrelations and a criterion-related validity study. *Journal of Research in Personality*, 44 (3), 315-327.
- Wainwright, M. J., & Jordan, M. I. (2008). Graphical models, exponential families, and variational inference. *Foundations and Trends in Machine Learning*, 1 (1-2), 1-305.
- Wirth, R. J., & Edwards, M. C. (2007). Item factor analysis: Current approaches and future directions. *Psychological Methods*, 12 (1), 5879.
- Woods, C. M., & Thissen, D. (2006). Item response theory with estimation of the latent population distribution using spline-based densities. *Psychometrika*, 71 (2), 281-301.

- Wu, M., Davis, R. L., Domingue, B. W., Piech, C., & Goodman, N. (2020). Variational item response theory : Fast, accurate, and expressive. *Educational Data Mining (EDM 2020)*, 1-12.
- Yalcin, I., & Amemiya, Y. (2001). Nonlinear factor analysis as a statistical method. *Statistical Science*, 16 (3), 275-294.
- Yates, A. (1988). *Multivariate exploratory data analysis: A perspective on exploratory factor analysis*. Albany, NY: State University of New York Press.
- Yun, J., Lozano, A. C., & Yang, E. (2020). A general family of stochastic proximal gradient methods for deep learning. *arXiv preprint*. Retrieved from <https://arxiv.org/pdf/2007.07484.pdf>
- Zhang, C., Butepage, J., Kjellstrom, H., & Mandt, S. (2019). Advances in variational inference. *IEEE Transactions on Pattern Analysis and Machine Intelligence*, 41 (8), 20082026.
- Zhang, S., Chen, Y., & Li, X. (2019). mirtjml [Computer software]. Retrieved from <https://cran.r-project.org/web/packages/mirtjml/index.html>
- Zhang, H., Chen, Y., & Li, X. (2020). A note on exploratory item factor analysis by singular value decomposition. *Psychometrika*, 1-15.
- Zhang, S., Chen, Y., & Liu, Y. (2020). An improved stochastic EM algorithm for large-scale full-information item factor analysis. *British Journal of Mathematical and Statistical Psychology*, 73 (1), 44-71.
- Zhou, D., Tang, Y., Yang, Z., Cao, Y., & Gu, Q. (2018). On the convergence of adaptive gradient methods for nonconvex optimization. *arXiv preprint*. Retrieved from <https://arxiv.org/pdf/1808.05671.pdf>

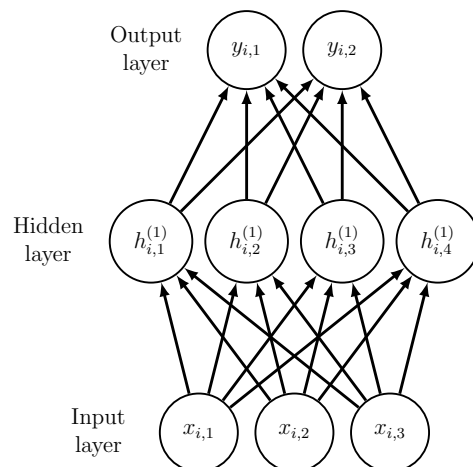
Figures

FIGURE 1.

Schematic representation of a feedforward neural network with a single hidden layer. The input layer is a 3×1 vector, the hidden layer is a 4×1 vector, and the output layer is a 2×1 vector.

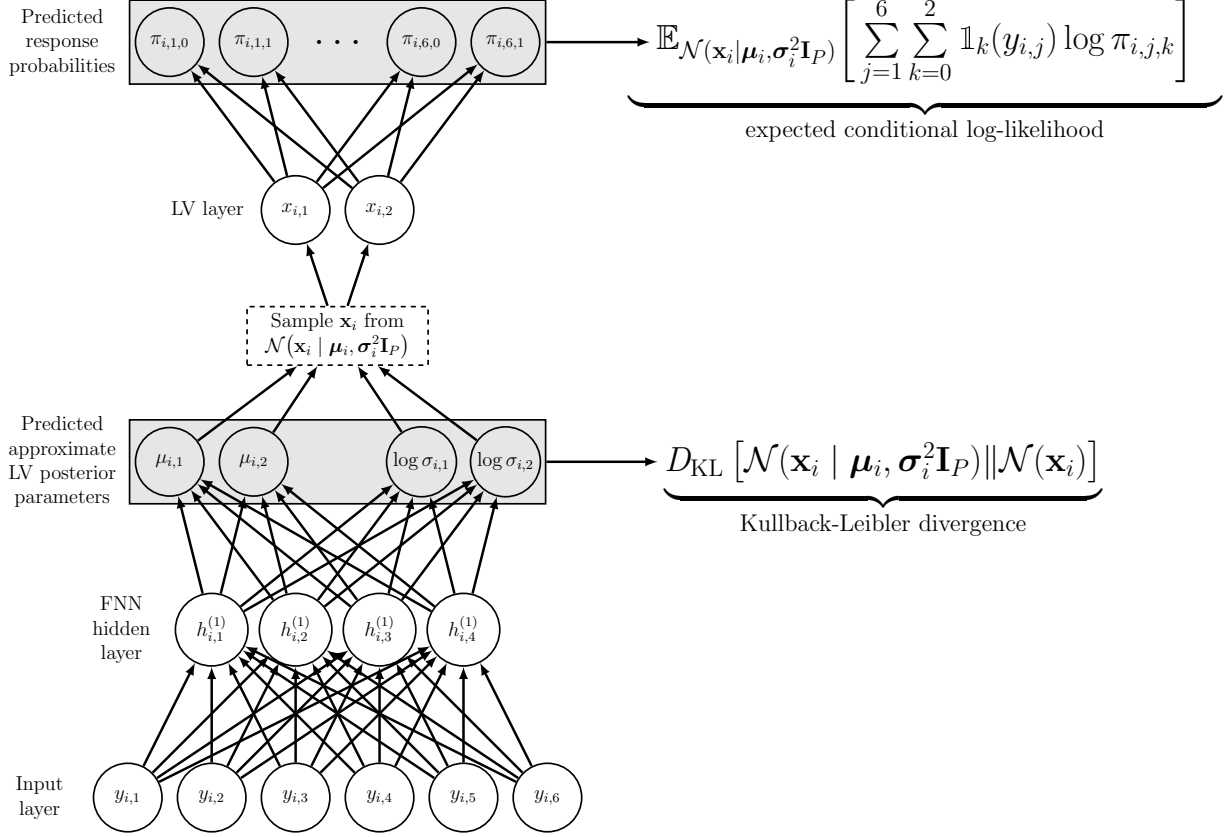


FIGURE 2.

Schematic diagram of a variational autoencoder for item factor analysis with $J = 6$ items, $C_j = 2$ categories per item, $P = 2$ factors, $S = 1$ Monte Carlo sample from the approximate latent variable posterior, and an inference model consisting of a feedforward neural network with a single hidden layer. The reparameterization trick is not illustrated for simplicity. LV = latent variable.

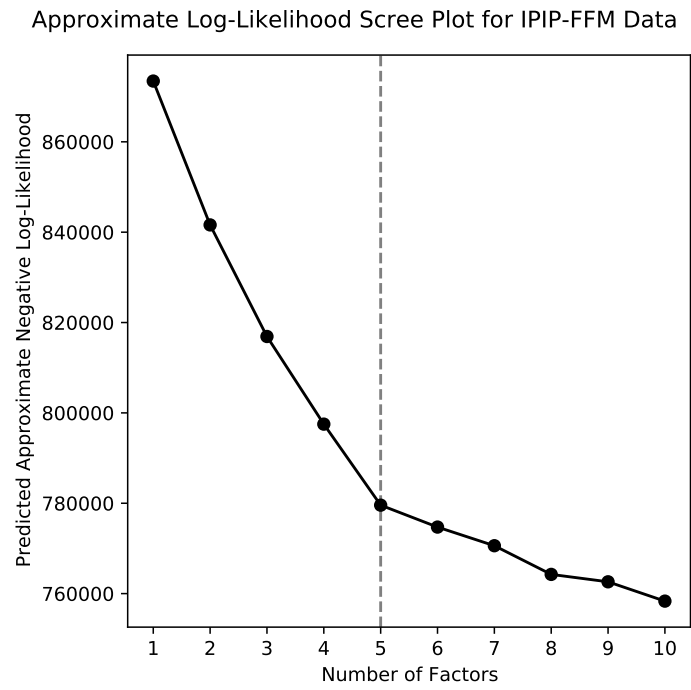


FIGURE 3.

Scree plot of predicted approximate negative log-likelihood as a function of the number of latent factors. The “elbow” at 5 factors is marked with a dotted line.

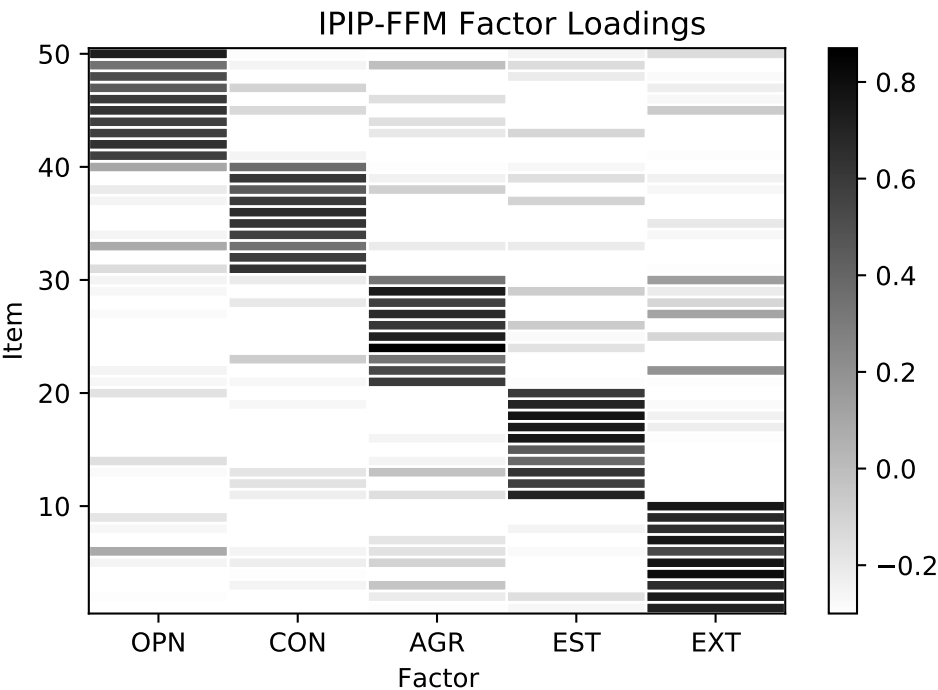


FIGURE 4.
Heat map of factor loadings for IPIP-FFM items. EXT = extraversion, EST = emotional stability, AGR = agreeableness, CON = conscientiousness, OPN = openness.

Asymptotic Bias for Amortized IWVI

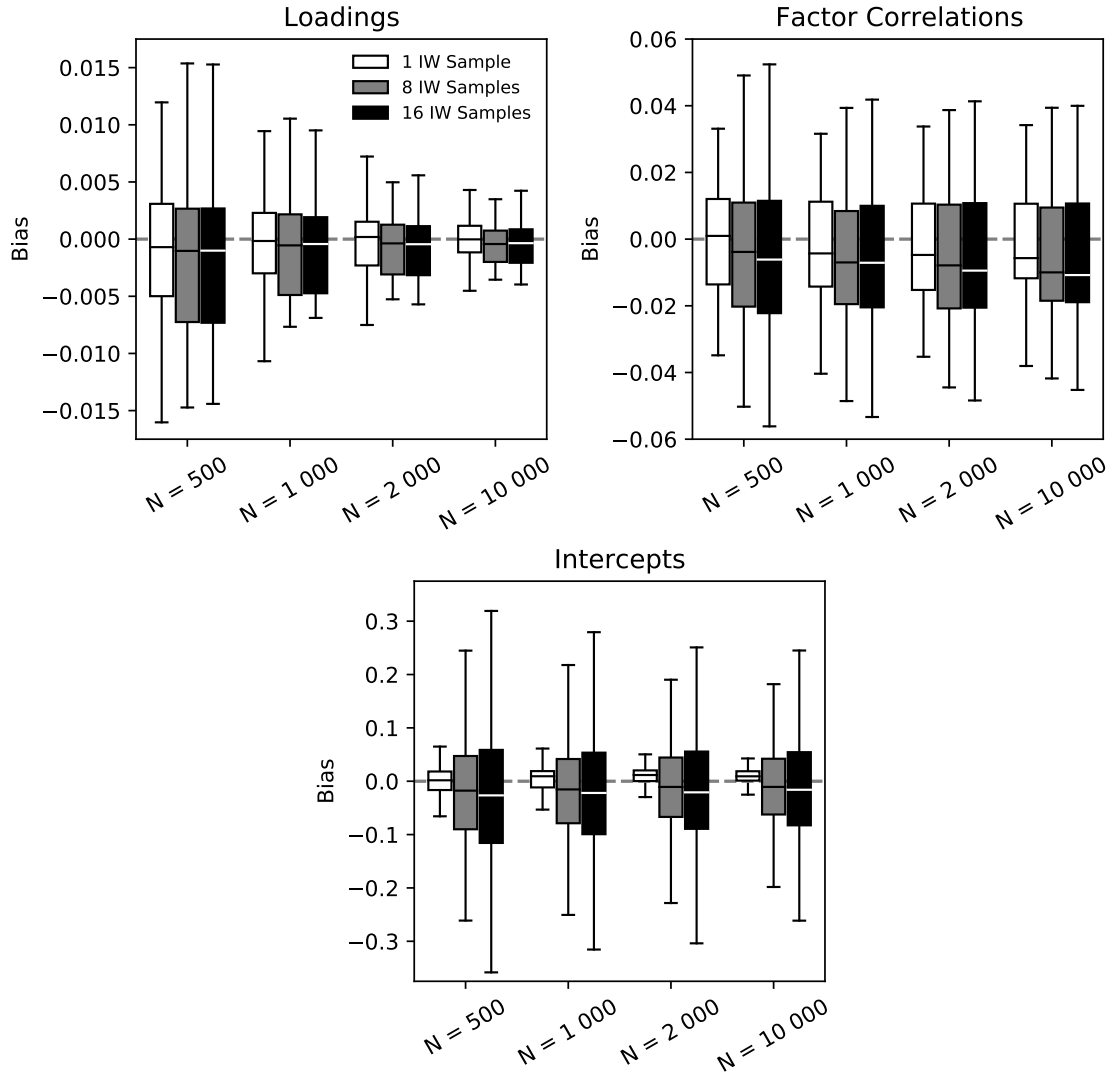


FIGURE 5.

Asymptotic parameter bias for the amortized importance-weighted variational estimator computed based on 100 replications of simulation. Three settings for the number of importance-weighted (IW) samples are compared. IWVI = importance-weighted variational inference.

Asymptotic Efficiency for Amortized IWVI

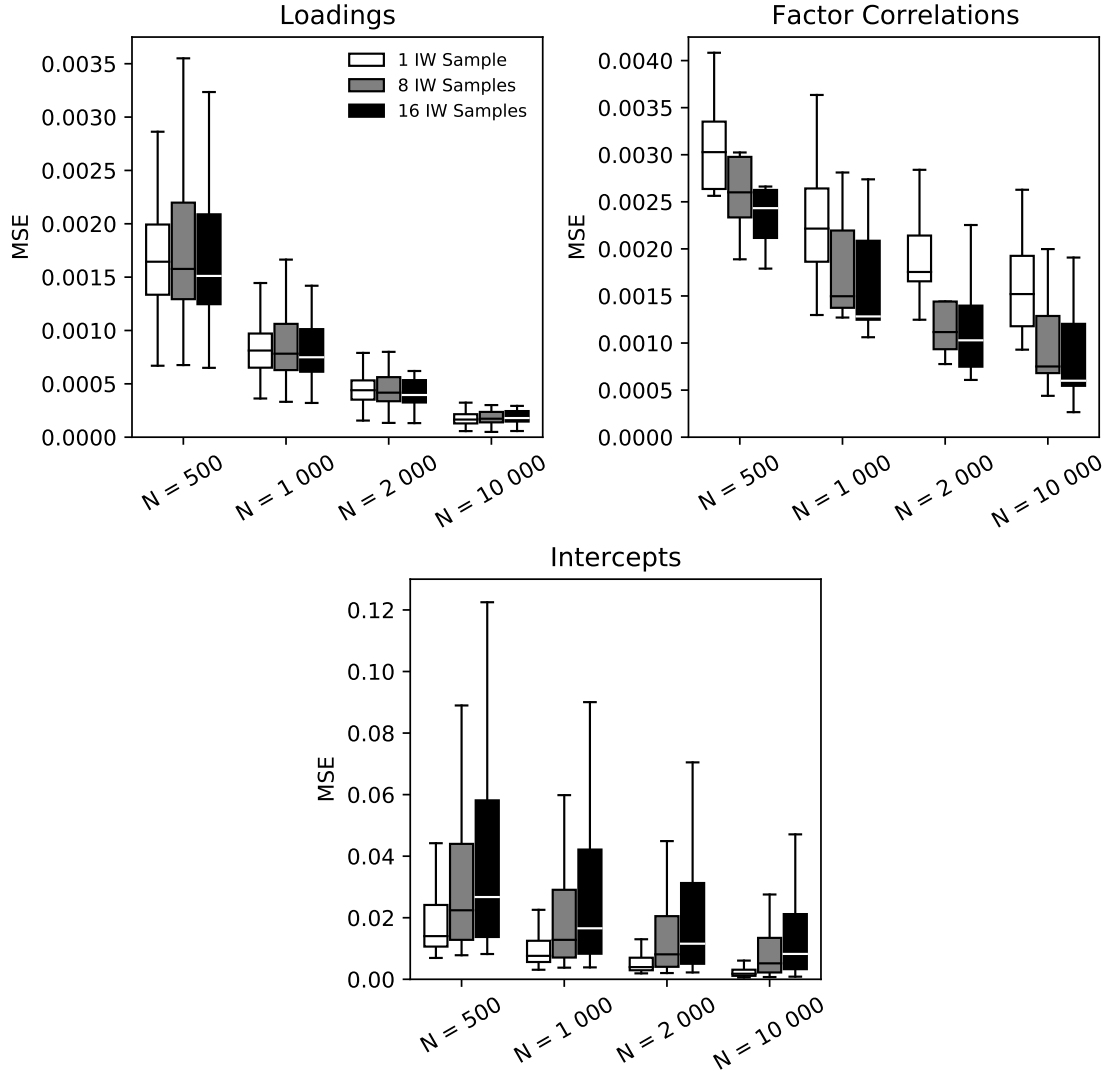


FIGURE 6.

Asymptotic parameter mean squared error (MSE) for the amortized importance-weighted variational estimator computed based on 100 replications of simulation.

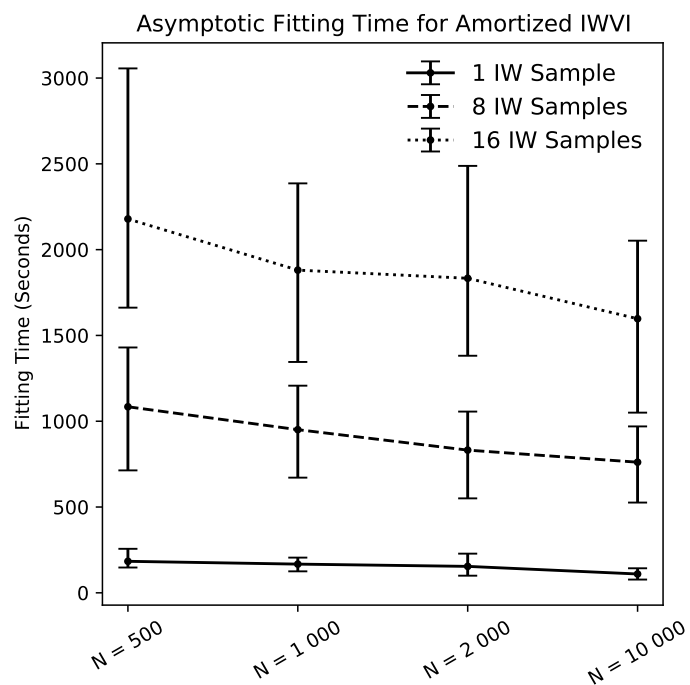


FIGURE 7.

Asymptotic fitting times for the amortized importance-weighted variational estimator across 100 replications of simulation. For all line plots in this work, points indicate median fitting times while error bars indicate 25% and 75% quantiles.

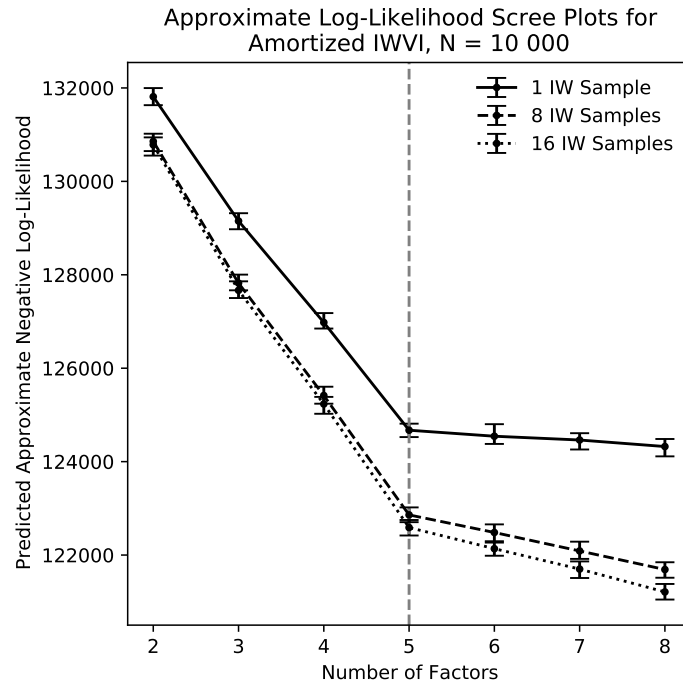


FIGURE 8.

Approximate log-likelihood scree plots for amortized IWVI constructed for simulation settings with $N = 10\,000$. The “elbows” at 5 factors are marked with a horizontal dotted line.

Asymptotic Efficiency for AVI Vs. MH-RM

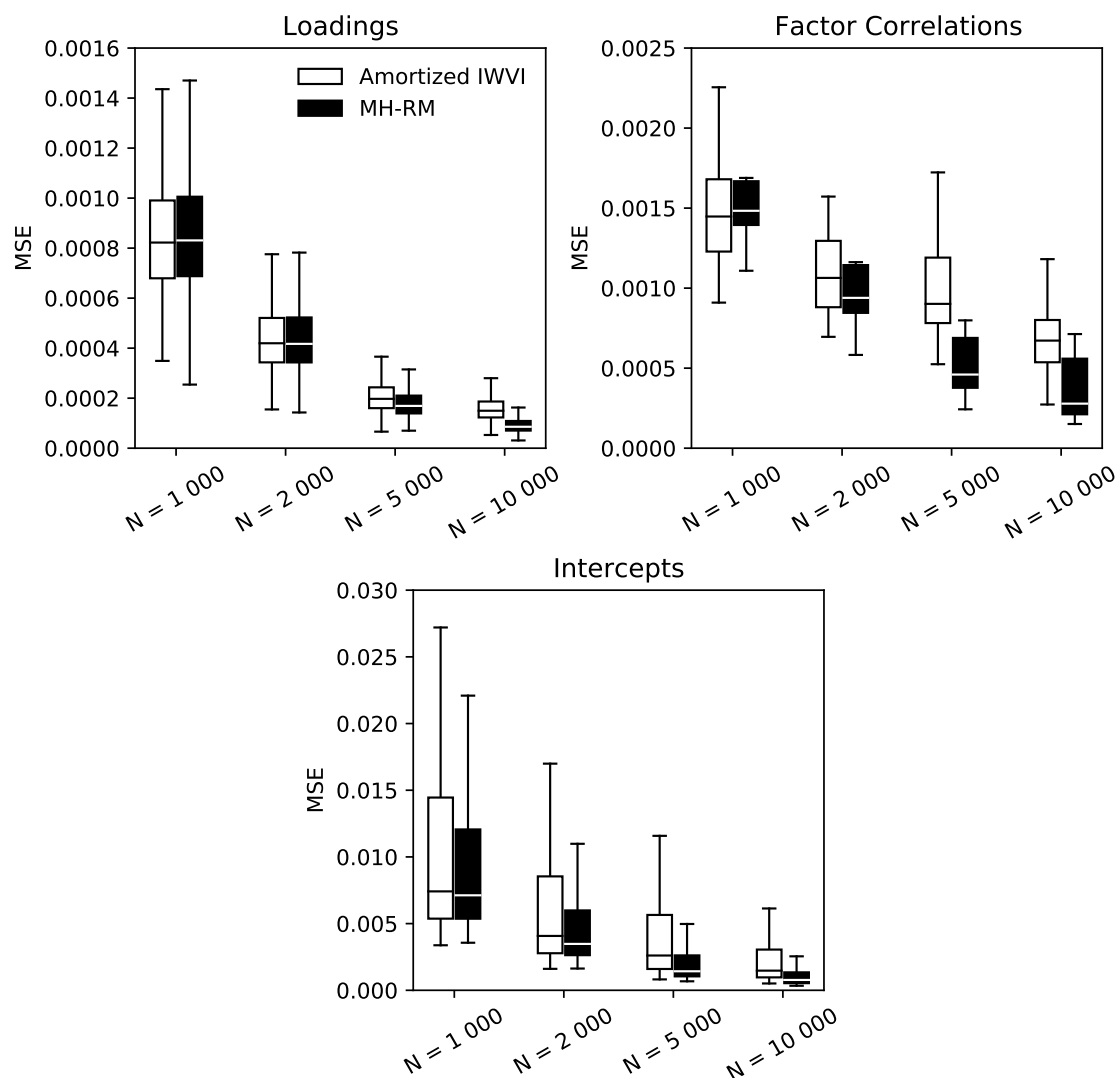


FIGURE 9.

MSE for the amortized variational estimator and the marginal maximum likelihood estimator computed based on 100 replications of simulation. AVI = amortized variational inference, MH-RM = Metropolis-Hastings Robbins-Monro.

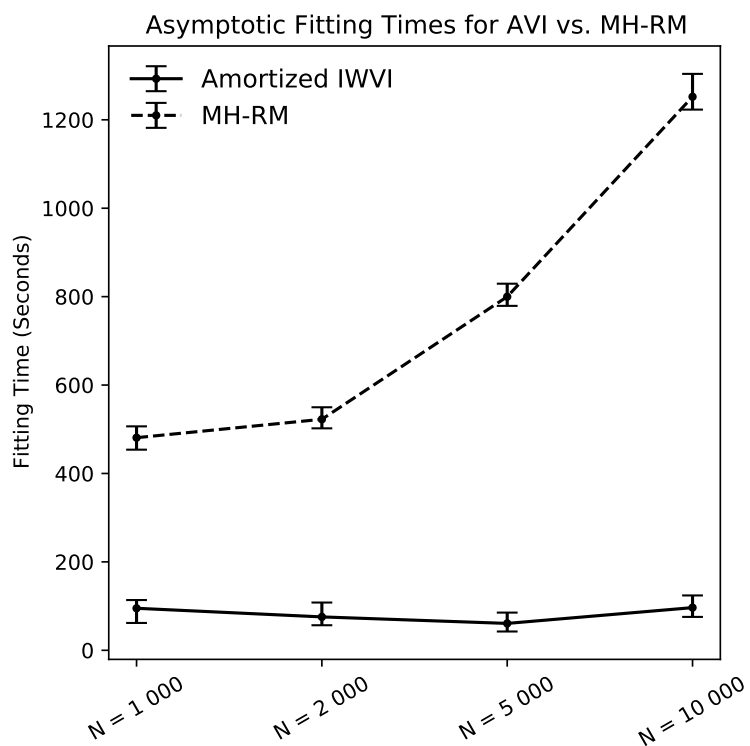


FIGURE 10.

Fitting times for the amortized variational estimator and the marginal maximum likelihood estimator computed based on 100 replications of simulation.

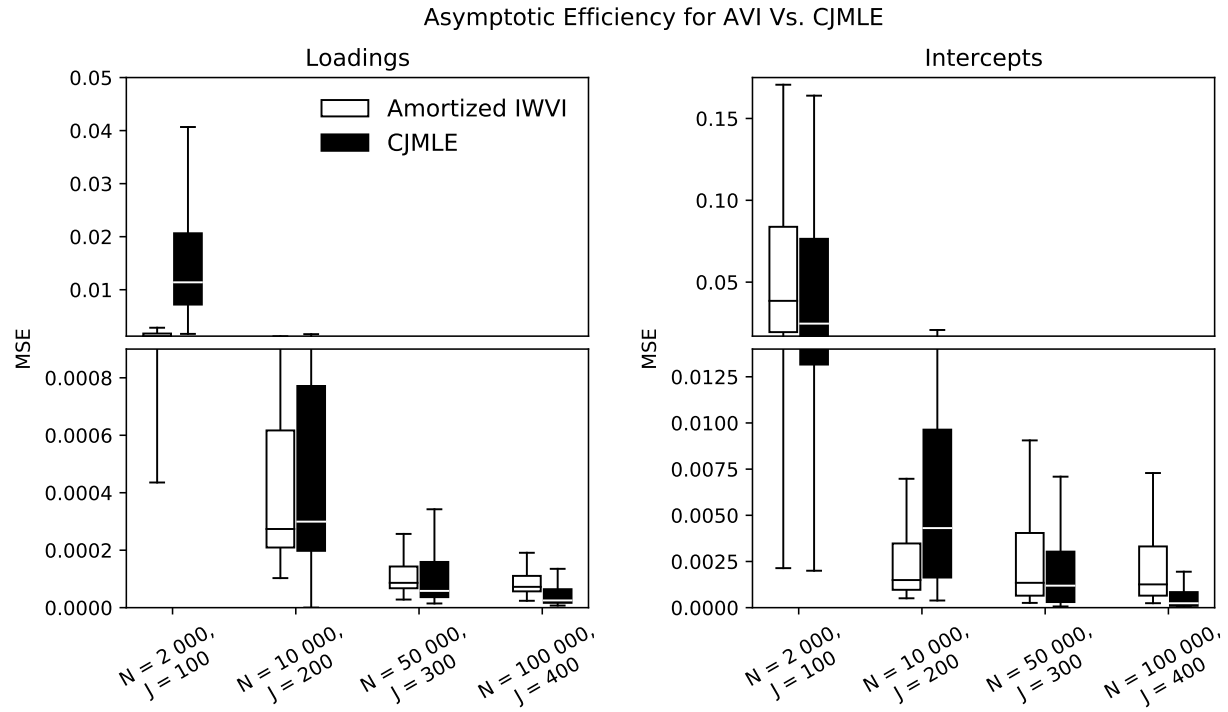


FIGURE 11.

MSE for the amortized variational estimator and the constrained joint maximum likelihood estimator (CJMLE) computed based on 100 replications of simulation.

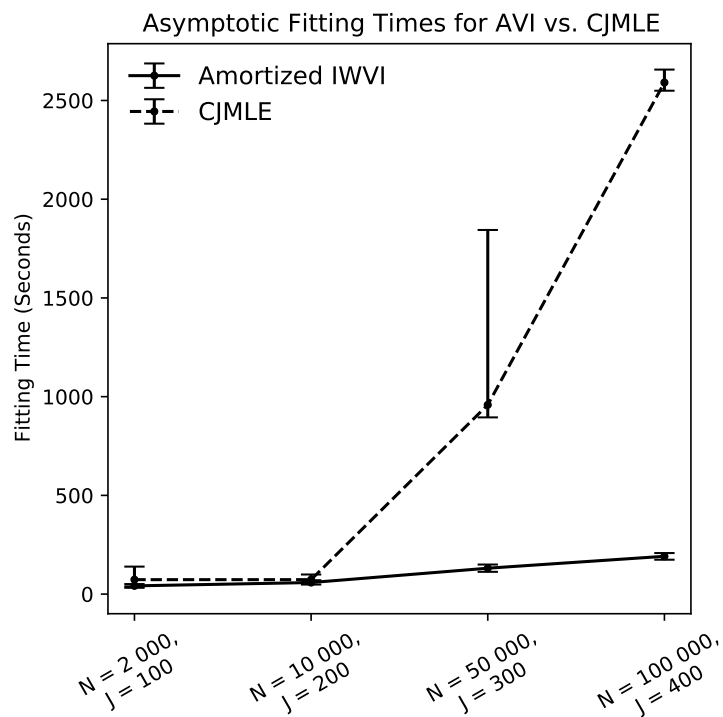


FIGURE 12.

Fitting times for the amortized variational estimator and CJMLE computed based on 100 replications of simulation.

Tables

TABLE 1.
Factor correlations for IPIP-FFM data set.

Factor	Factor				
	1	2	3	4	5
1. Extraversion	1.00				
2. Emotional Stability	-.18	1.00			
3. Agreeableness	.16	-.01	1.00		
4. Conscientiousness	.11	-.11	.06	1.00	
5. Openness	.17	-.08	.08	-.01	1.00

Algorithms

Algorithm 1 *Deep Learning Algorithm for Exploratory Item Factor Analysis*

1. **Initialization** Input item responses \mathbf{Y} ; dimension of latent space P ; mini-batch size M ; importance-weighted samples R ; Monte Carlo samples S ; optimization hyperparameters η , β_1 , and β_2 ; and starting values $\boldsymbol{\xi}_0 = (\boldsymbol{\theta}_0^\top, \boldsymbol{\phi}_0^\top)^\top$
 2. At fitting iteration t , $t = 0, \dots, T$:
 - (a) **Computation** Randomly sample a mini-batch $\{\mathbf{y}_i\}_{i=1}^M$; compute objective function value for respondent i , $i = 1, \dots, M$:

$$(\boldsymbol{\mu}_i^\top, \log \boldsymbol{\sigma}_i^\top)^\top = \text{FNN}_{\boldsymbol{\phi}_t}(\mathbf{y}_i)$$
for $r = 1, \dots, R$, $s = 1, \dots, S$:

$$\boldsymbol{\epsilon}_{i,r,s} \sim \mathcal{N}(\boldsymbol{\epsilon}_{i,r,s})$$

$$\mathbf{x}_{i,r,s} = \boldsymbol{\mu}_i + \boldsymbol{\sigma}_i \odot \boldsymbol{\epsilon}_{i,r,s}$$

$$\log p_{\boldsymbol{\theta}_t}(\mathbf{y}_i \mid \mathbf{x}_{i,r,s}) = \sum_{j=1}^J \sum_{k=0}^{C_j-1} \mathbb{1}_k(y_{i,j}) \log \pi_{i,j,k}$$

$$D_{\text{KL}}[\mathcal{N}(\mathbf{x}_{i,r,s} \mid \boldsymbol{\mu}_i, \boldsymbol{\sigma}_i^2 \mathbf{I}_P) \parallel \mathcal{N}(\mathbf{x}_{i,r,s})] = \frac{1}{2} \sum_{p=1}^P [\mu_{i,p}^2 + \sigma_{i,p}^2 - 1 - \log \sigma_{i,p}^2]$$

$$w_{i,r,s} = \exp \left[\log p_{\boldsymbol{\theta}_t}(\mathbf{y}_i \mid \mathbf{x}_{i,r,s}) - D_{\text{KL}}[\mathcal{N}(\mathbf{x}_{i,r,s} \mid \boldsymbol{\mu}_i, \boldsymbol{\sigma}_i^2 \mathbf{I}_P) \parallel \mathcal{N}(\mathbf{x}_{i,r,s})] \right]$$
end for

$$\text{IW-ELBO}_i \approx \frac{1}{S} \sum_{s=1}^S \left[\log \frac{1}{R} \sum_{r=1}^R w_{i,r,s} \right]$$
 - (b) **Optimization** Update model parameters using AMSGrad:

$$\mathbf{g}_t = \frac{1}{M} \nabla_{\boldsymbol{\xi}_t} \sum_{i=1}^M \text{IW-ELBO}_i$$

$$\mathbf{m}_t = \beta_1 \mathbf{m}_{t-1} + (1 - \beta_1) \mathbf{g}_t$$

$$\mathbf{v}_t = \beta_2 \mathbf{v}_{t-1} + (1 - \beta_2) \mathbf{g}_t^2$$

$$\hat{\mathbf{v}}_t = \max(\hat{\mathbf{v}}_{t-1}, \mathbf{v}_t)$$

$$\boldsymbol{\xi}_{t+1} = \boldsymbol{\xi}_t - \eta \frac{\mathbf{m}_t}{\sqrt{\hat{\mathbf{v}}_t}}$$
 3. **Output** Return $\hat{\boldsymbol{\xi}} = \boldsymbol{\xi}_T$
-